We are IntechOpen,
the world's leading publisher of
Open Access books
Built by scientists, for scientists

4,800
Open access books available

122,000
International authors and editors

135M
Downloads

Our authors are among the

154
Countries delivered to

TOP 1%
most cited scientists

12.2%
Contributors from top 500 universities

CLARIVATE ANALYTICS
BOOK CITATION INDEX
INDEXED

WEB OF SCIENCE™

Selection of our books indexed in the Book Citation Index
in Web of Science™ Core Collection (BKCI)

Interested in publishing with us?
Contact book.department@intechopen.com

Numbers displayed above are based on latest data collected.
For more information visit www.intechopen.com

Electrodeposition of Insulating Thin Film Polymers from Aliphatic Monomers as Transducers for Biosensor Applications

Guillaume Herlem and Tijani Gharbi
Institute FEMTO-ST/Department of Optic, UMR CNRS 6174,
University of Franche-Comte
France

1. Introduction

Molecules can be oxidized anodically or reduced cathodically depending on their chemical functions but only some of them can be electropolymerized. The electropolymerization process of organic molecules leading to conductive, semiconducting or insulating polymer takes place at the surface of a biased electrode. In this case, a modification of an electrode surface, that can be a semiconductor or a conductive one, occurs in an irreversible way.

Electrodes coated with conducting polymer films, have attracted considerable interest in the last two decades. A multitude of reviews and monographs have been written on the subject (Adhikari et al., 2004). Many electrochemical works were performed with aromatic or conjugated compounds yielding insulating polymer too. But few studies were made up to now with aliphatic molecules concerning their electropolymerization behavior. One of the reasons comes from the problem to study thin film which requires characterizations with expansive and not widespread spectroscopic analysis methods such as x-ray photoelectron spectroscopy and AFM imaging for instance. Furthermore, thin coatings at the electrode surface which could occur during a reaction, were neglected for a long time and regarded as a baneful interference hushing a possible insulating polymer up.

Electropolymerized thin film polymers possess a wide range of applications in electroanalysis (Kalimuthu et al., 2009), energy storage (Granqvist, 2007), electrocatalysis (Xiao et al., 2009), biosensing (Merkoci, 2009), corrosion protection (Medrano-Vaca et al., 2008), sensors and electronic devices (Liu et al., 2010), electrochromic displays (Reiter et al., 2009), etc. Although polymer films on a surface can be formed in several chemical ways, electropolymerization is one of the most convenient and advantageous especially the thickness control during the film growth.

On one hand, poly(thiophene), poly(pyrrole), poly(aniline) and their derivatives are amongst the most widely studied conducting polymers. This is probably due to the high conductivities of their oxidized forms and their ability to reversibly switch between conducting and insulating states by doping and undoping. On the other hand, insulating polymers have not paid so much attraction. Their electrochemical growth on an electrode surface is limited to thin film especially for aliphatic molecules due to the resulting current drop. If their thickness does not reach more than tens of nanometers, the surface electrode is

modified durably and uniformly. But advantageous properties such as biocompatibility or proton affinity for these polymers compared to previous ones will be of prime importance for sensor and biosensor applications.

Consequently, the aim of this chapter is to draw up recent research studies concerning the electrochemistry of aliphatic molecules leading to thin film polymer coatings. These thin film are of interest in sensor and biosensor developments as we can see further.

2. Electrochemistry of bi-functional aliphatic molecules

The origin of the work concerning the electropolymerization of aliphatic bifunctional molecule comes back to the study of simple ω-amines which are known to form aminates (analog to hydrates' name) which are highly conductive electrolytes (Herlem et al. 2000). Despite the potential window of primary amines (about 3.5 V on platinum electrode), ethylenediamine (EDA) shown abnormal electrochemical behavior when biased anodically. In this case the electrode passivation occurs. This is the reason why we studied amine compounds with great interest. In addition, some combinations have been made with different functional groups as shown of the Figure 1.

$$A \overbrace{\left(CH_2 \right)}_{n} B$$

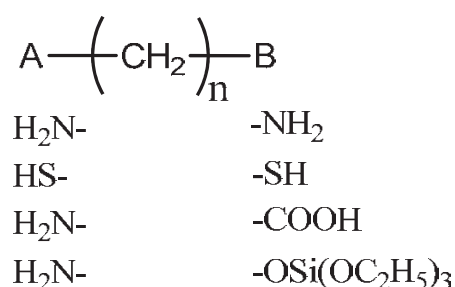| H$_2$N- | -NH$_2$ |
HS-	-SH
H$_2$N-	-COOH
H$_2$N-	-OSi(OC$_2$H$_5$)$_3$

Fig. 1. Bifunctional molecule with a combination of groups A and B leading to electrodeposition.

The choice of the functional groups depicted Figure 1 was done in the light of some observations made concerning substituted ω-amines. This is also an attempt to generalize the particular electrochemical behavior of some bifunctional aliphatic molecules which can be electropolimerized.

In a first part, a description of the electrochemistry of ω-amine based electrolytes will be given, followed with the electrochemical behavior of ethanedithiol. Then, in a third part, we will discuss on the electrochemistry of concentrated glycine based electrolytes. At last, we will see in which conditions the electrodeposition of 3-aminopropyltriethoxy silane occurs.

2.1 Anodic oxidation of primary di and tri amines

It was pointed out previously that the passivation of electrodes such as smooth platinum and gold, titanium and glassy carbon occurs during the anodic oxidation of an electrolyte composed with one salt dissolved in one pure di or tri amine. The originality resides here in the use of the solvent which is also the monomer. No co-solvent has to be added in the electrolyte because of the good solubility of salts and the excellent conductivities reached. The electrode passivation only occurs with unsubstituted primary di and tri amines H$_2$N-(CH$_2$)n-NH$_2$ where primary amino groups are at the two ends of the alkyl chain (Herlem et al., 1999). The method of choice underlying this phenomenon is the electrochemical quartz

crystal microbalance (EQCM) technique coupled to cyclic voltammetry measurement (Figure 2):
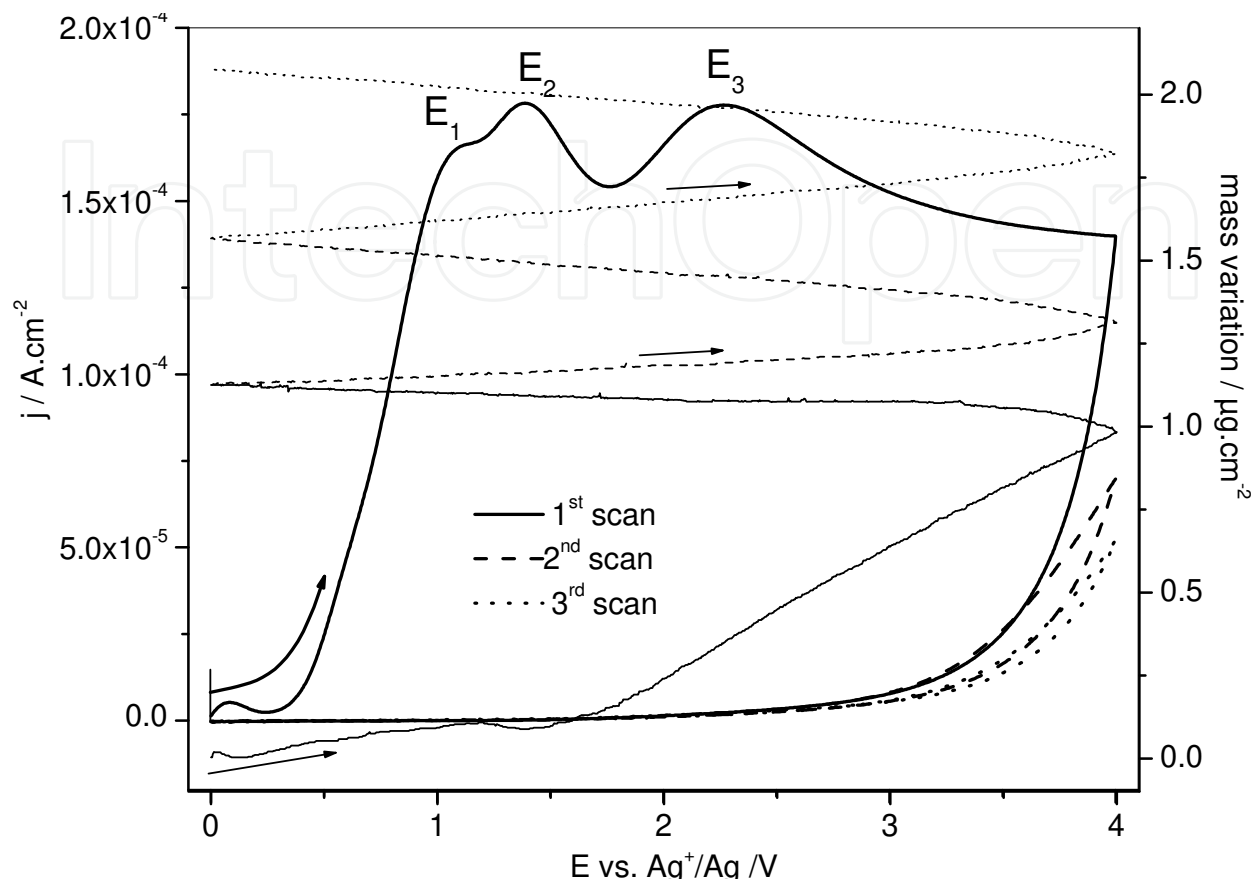

Fig. 2. Mass variation coupled to cyclic voltammetry of 1,3-DAP charged with KPF6 0.1 M on 5 MHz Au quartz coated electrode (scan rate: 20mV/s, counter-electrode: Pt, reference electrode: Ag wire).

During the first scan, as soon as the anodic peak E2 at +1.4 V is reached, the mass increases at the electrode surface as shown Figure 2. This is the case for 1,3-diaminopropane (1,3-DAP) based electrolytes and observed experimentally for EDA and diethylenetriamine (DETA) based electrolytes too. Beyond 3V, there is a plateau where the current is constant. At the second scan (and also for the next ones) there is a drastic drop of current density. All the peaks have disappeared but the mass deposition still increases. The broadness of the peaks on the voltammograms (E1=1.1 V, E2= 1.4 V, E3= 2.2 V vs. Ag+/Ag for 1,3-DAP) are characteristic of the electrochemical behavior of primary amines. Notice that for 1,4-diaminobutane and other diamines with increasing alkyl length chain between the two amino groups, the melting points are decreased drastically.

The electropolymerization process of primary di or tri amines is possible on different metallic or semiconducting electrodes such as smooth gold, smooth platinum, glassy carbon, p or n-type silicon, Fluorine Tin Oxide (FTO). It does not happen with Iron or Copper electrodes for instance. Copper and silver cations are known to be remarkably chelated by EDA and consequently the corresponding metals are oxidized anodically at a lower potential than those of EDA or DETA. From the HSAB principle from Parr and Pearson, metallic copper electrode cannot be used as working electrode in amine based electrolytes

because of its cationic hardness which is very close to that of the amine giving a reaction between the two species (Table 1).

	Cu+	Ag$^+$	Pt^{2+}	Pt	EDA	1,3-DAP	DETA
η (eV)	6.3	7	8.0	3.5	6.2	6.3	6

Table 1. Chemical hardnesses of Pt and some metallic ions and amines calculated at the Hartree-Fock level of theory using 6-31G basis sets.

On the other hand, the hardness value of Pt^{2+} means that Pt will not be ionized anodically and complexed by the amines having lower hardness value. This is one of the reasons why noble metals like Pt are used in the electrochemistry of amines for example.

Two parameters have to be taken into accounts that prevent the electropolymerization of the primary di or triamines during their anodic oxidation. First, amines based electrolytes must be anhydrous. Addition of water in these media dramatically modify the voltammograms by generating an anodic wall, instead of the plateau observed previously, that appears at a lower potential particularly as the water concentration increases (Figure 3).
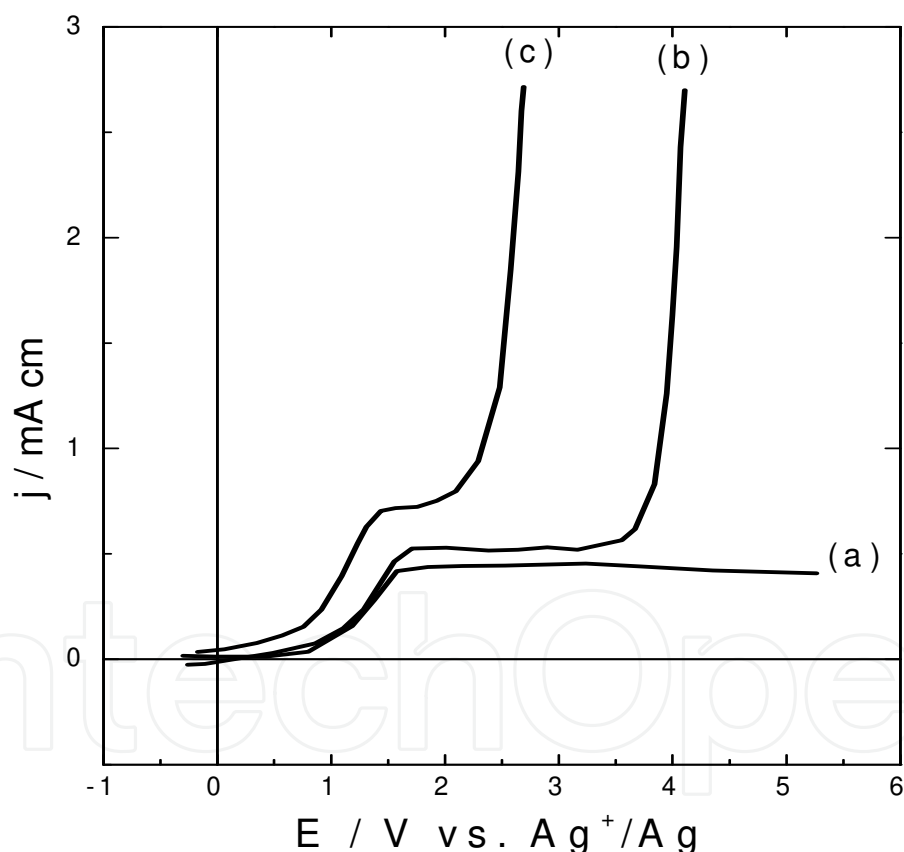

Fig. 3. Electrochemical behavior (reverse scans are not presented) of a smooth Pt electrode in pure EDA vs. Ag+/Ag, as a function of increasing quantity of water (supporting electrolyte: LiSO2CF3 0.1 M; Scan rate 10mVs-1).(a) : 0 % of water. (b) : 17 % of water. (c) : 29 % of water.

Secondly, the anodic oxidation takes place only with primary amines and the vicinal carbon does not have to be substituted. The resulting thin films are insoluble in various solvents as cold water, acetone, propylene carbonate, ethanol, ω-alkylamine, etc, modifying durably the electrochemical behavior of the electrode.

Spectroscopic analysis such as FT-IR (Fourier Transform-Infrared), IRAS (Internal Absorption), IR-ATR (Attenuated Total Reflection), Raman and XPS (X-Ray Photoelectron spectroscopy) revealed the polymeric structure of the thin film coating during the anodic oxidation of an ω-alkylamine. For instance, ethylenediamine leads to linear polyethylenimine (L-PEI) while 1,3-DAP gives linear polypropylenimine (L-PPI). DETA, which is the dimer of EDA, induces L-PEI too.

IR-ATR spectra from electropolymerized and from organic synthesized L-PEI (and L-PPI) fit in good agreement each other's (Saegusa et al., 1972), (Biçak et al., 1998), (). ν(NH): 3200-3400 cm^{-1}, ν(CH$_2$): 2800-2950 cm^{-1}, ν(NH): 1450-1600 cm^{-1}, δ(CH): 1300-1450 cm^{-1}, ν(C-NH-C): 1050-1150 cm^{-1}. Wavelength number values can fluctuate because of the mass weight variations of the polymers depending on the experimental conditions in particular the bias time.

Raman spectroscopy discarded, from the mechanism, a possible formation of substituted hydrazine(s) due to the doubling of the radical formed after the loss of a proton and an electron.

XPS spectra of L-PEI coating from EDA electropolymerization match well those already published (Beamson et al., 1992). C1s and N1s peaks at BE = 285.7 eV and 399.7 eV respectively corresponds to the C-N bond in –CH$_2$-CH$_2$-N– pattern. XPS confirms also the presence of –C=N– and –C=O bonds in a small extent located at the surface electrode.

Spectroscopic results from the electropolymerized polyalkylenimine can be compared to those synthesized via organic chemistry. Linear polyethyleneimine (L-PEI) was first synthesized by chemical route in 1970 by Dick (Dick et al., 1970). L-PEI can be obtained by the cationic polymerization of 2-substituted-2-oxazolines or by aqueous polymerization of aziridine (Gembitskii et al., 1978) but the electrochemical synthesis is far less complicated than the organic one.

In the light of ab initio calculations, the probable mechanism for the anodic oxidation of EDA described elsewhere (Lakard et al., 2002) is essentially as shown in Figure 4. The reaction, based on studies by Mann and others (Mann et al., (1970), consists of the monomer adsorption on the electrode surface in the two first steps. In a third step there is the monomer oxidation with a departure of one electron followed, in a fourth step, by the cleavage of the C-N bond. The fifth step is the attack of another ω-amines by the former primary carbocation. The following steps are the expulsion of the proton from the protonated amine, a loss of one electron like in step 3 and then the breaking of the C-N bond like in step 4. Step 5 can goes on to give the chain growth.

2.2 Anodic oxidation of ethanedithiol

According to Figure 1, another interesting bifunctional molecule is 1,2-ethanedithiol (EDT) (Lakard et al., 2008). Its electrochemical behavior was studied by mean of cyclic voltammetry in anodic oxidation. Although EDT is liquid at ambient temperature, conducting salts are insoluble and EDT was dissolved in a co-solvent. In acetonitrile Figure 5 a typical cyclic voltammogram shows two peaks at 1.79 V and 2.16 V versus Ag$^+$/Ag, but only during the first scan. During additional scans, the oxidation peaks are less pronounced but the anodic peaks remains nearly the same from one scan to other. These observations underline that EDT is oxidized under anodic potentials leading to the electrode passivation. Electrochemical Quartz Crystal Microbalance experiment performed on a Pt coated quartz shows Figure 6 that it is not necessary to scan out to a potential greater than 3 V vs. Ag+/Ag since the film grows after the second oxidation peak.
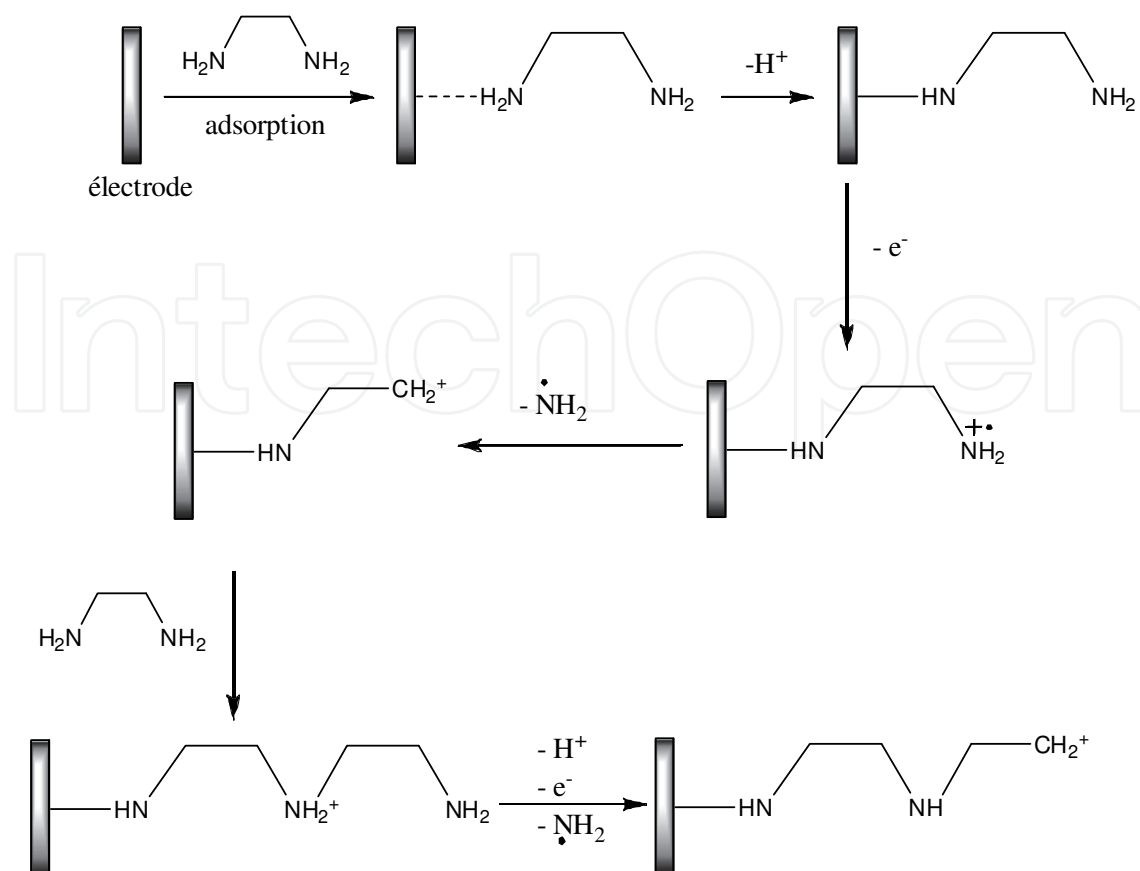
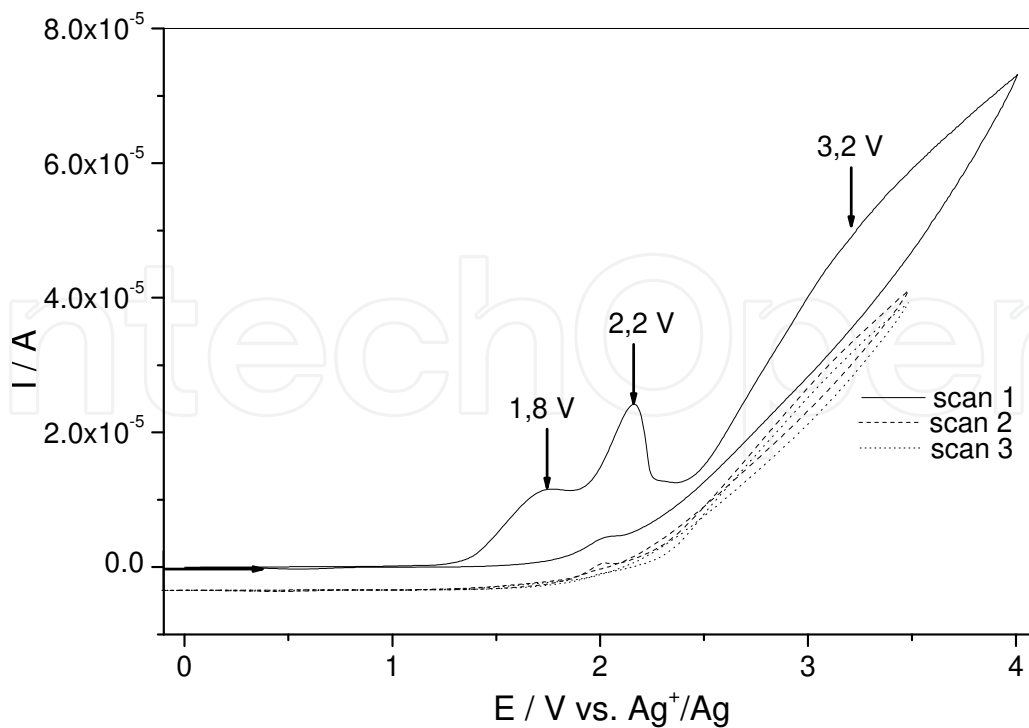Fig. 4. Anodic oxidation mechanism of EDA

Fig. 5. Cyclic voltammogram of EDT 2.34M charged with LiTFSI 1 mM in acetonitrile on Pt. Scan rate: 20 mV/s.
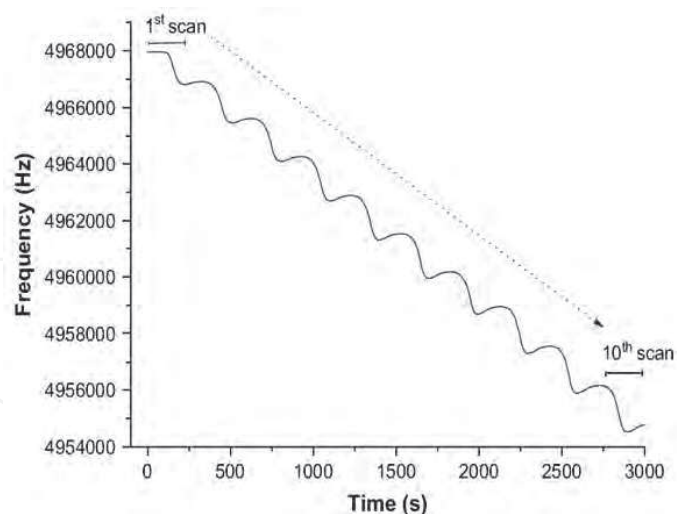
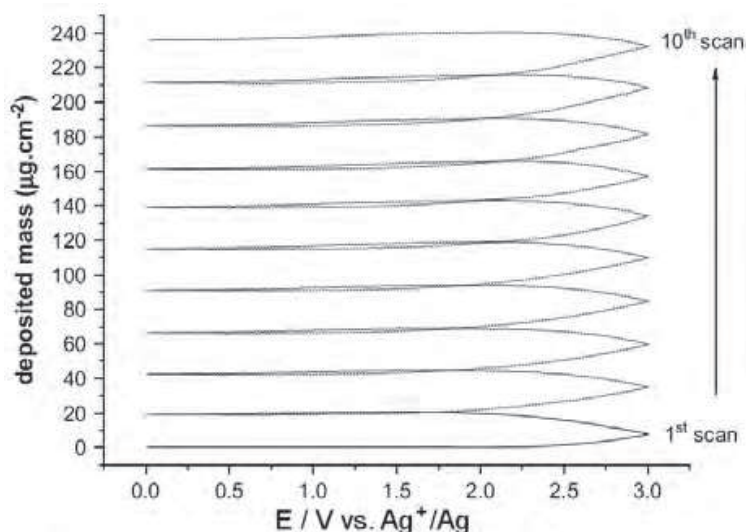Fig. 6. Frequency changes as a function of time during the anodic oxidation of EDT.

Fig. 7. Frequency changes as a function of the potential during the anodic oxidation of EDT

From the Figure 6 it can be observed also that the oxidation of EDT leads to a general decrease of the platinum-coated quartz frequency. The deposited mass on the electrode surface as a function of the potential is displayed Figure 7. The weight increase is observed at the second peak (2.16 V) of the first cycle. The deposited mass continues to increase as far as the potential is superior to 2.0 V. It can be noticed too that the deposited mass increases for subsequent scans and that the deposited mass is about the same for each cycle. So, the film synthesized at the electrode surface grows as much as repeated cycles.

X-ray photoelectron, Raman and IR analysis, were made on films deposited on platinum electrodes by anodic oxidation of EDT in acetonitrile charged with LiTFSI. Even after rinsing by pure water and ethyl alcohol, then drying under vacuum, the surface of the coating showed the presence of the supporting salt LiTFSI as shown by one O1s peak at a binding energy of 535.0 eV and one N1s peak at 403.9 eV (Figure 8a). Moreover, the XPS spectrum indicates that oxidized EDT gave one C1s peak at 288.5 eV, one S2s peak at 231.0 eV and two S2p3/2 peaks 165.3 eV and 164.0 eV (these binding energies fit well with those already

published (Rosado et al., 1998; Taga et al., 1997). Figure 8bcd shows narrow range scans for C1s, S2s and S2p3/2, respectively. Comparing these binding energies with those already published, it can be deduce that C1s peak is indicative of C-C or C-S bonds, that S2p3/2 peaks at 165.3 eV and 164.0 eV correspond to S-S bond and C-S bond of R-S-S-R molecule, respectively, and that the C/S atomic ratio deduced from XPS intensities is 1 for the film formed by oxidation of EDT.
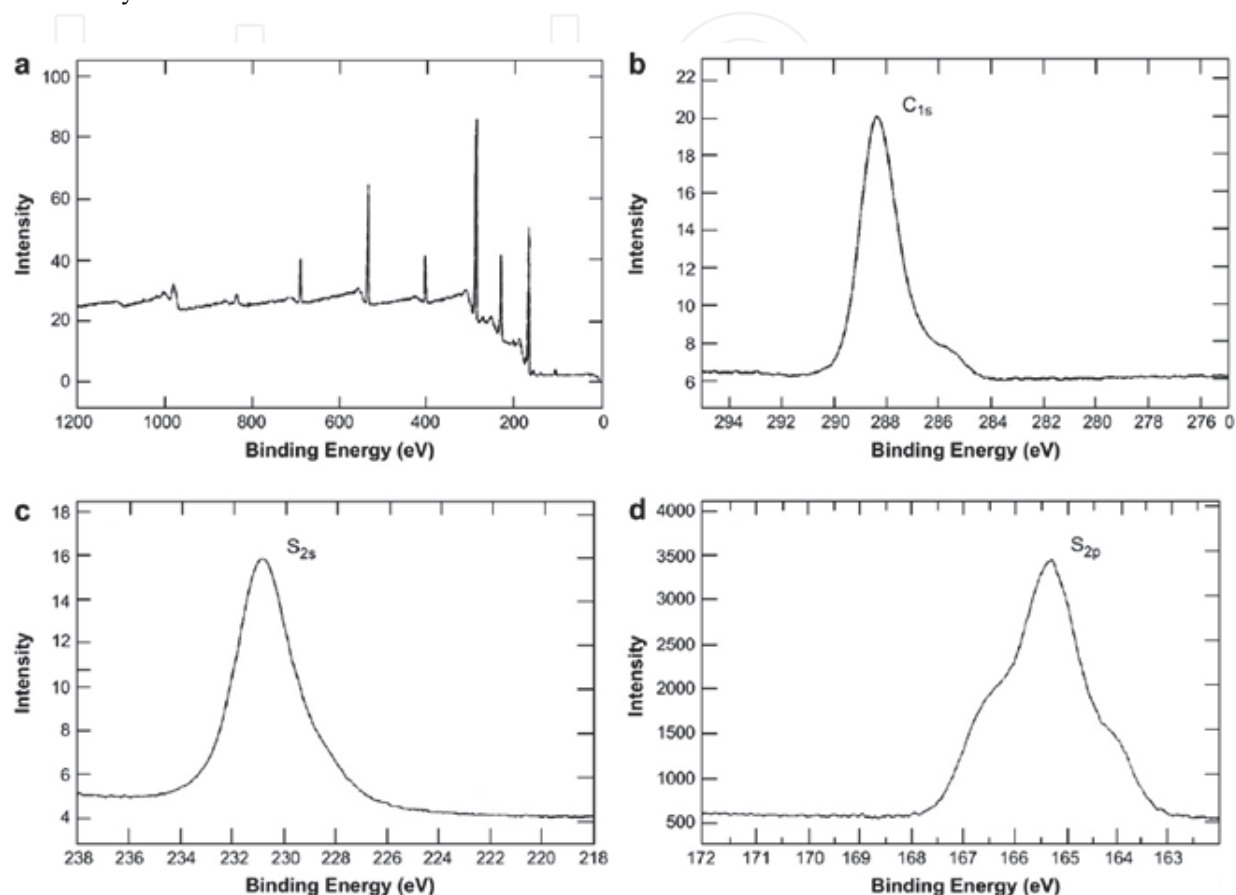

Fig. 8. xps spectra of anodically oxidazed EDT on smooth platinum.

Raman spectra from oxidized EDT gave additional information about the electrosynthesized films on the platinum electrode surfaces. A typical spectrum of the resulting film from the anodic oxidation of EDT in acetonitrile is shown Figure 9. Some characteristic vibration bands of polydisulfides can be underlined: asymmetric and symmetric -CH stretching modes at 2948 and 2904 cm^{-1}, respectively, -CH deformations at 1410 and 1280 cm^{-1}, C-C stretching at 1051 cm^{-1}, C-S out of plane vibration band at 731 cm^{-1} and S-S stretching at 505 cm^{-1}. No SH vibration band was observed between 2500 and 2600 cm^{-1}.

IRRAS spectroscopy (Figure 10) confirms Raman and XPS analyses. The main characteristic vibration bands of the polysulfide film are: -CH deformation at 1410 cm^{-1} and 1260 cm^{-1}, C-S vibration bands at 1200 cm^{-1} and 1100 cm^{-1} and C-S out of plane vibrations at 700 cm^{-1}. These peaks fit well with those obtained from similar compounds such as polyethylenesulfide or polypropylenesulfide. We could also notice that no -SH vibration band was observed in the IRRAS spectra (localized between 2500 and 2600 cm^{-1}).

From these spectroscopic studies, the product of anodic oxidized EDT leads to a polyethylenedisulfide film whose structure is similar to $(S-S-CH_2-CH_2)_n$.
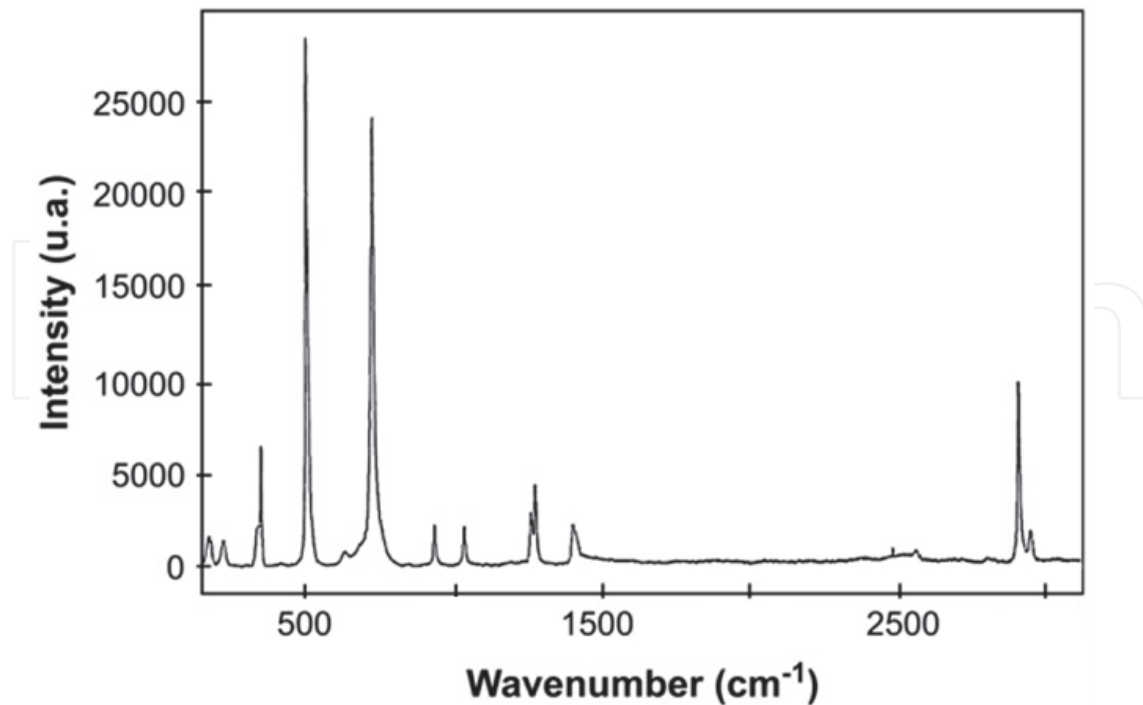
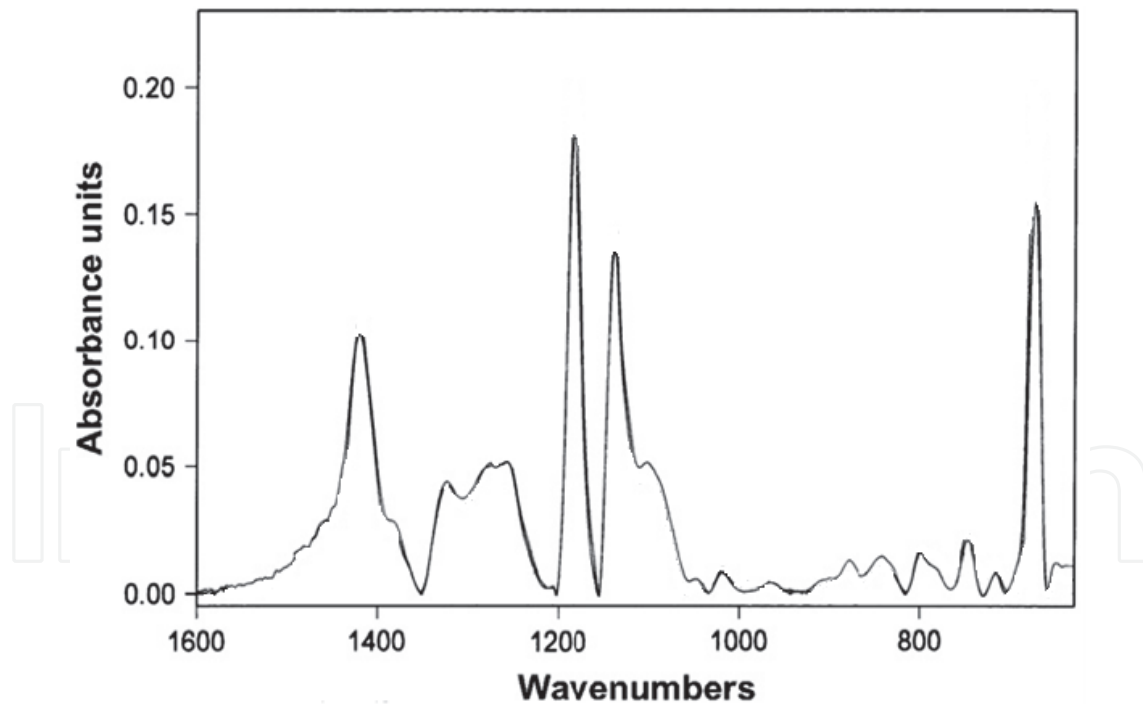Fig. 9. Raman spectrum of oxidized EDT modified platinum surface.

Fig. 10. IRRAS spectrum of oxidized EDT modified platinum surface.

Previous studies (Svensmark et al., 1991) on the electrochemical oxidation of thiols and related compounds on noble metal electrodes have shown that the electrochemical oxidation process of a thiol, noted R-SH, involves the initial formation of the $RS^{+\bullet}$ radical cation, followed by the formation of the $RS^{\bullet}$ radical and by the dimerization to the disulfide. This reaction was used as the first steps of the proposed mechanism (Figure 11). The first step is

adsorption of monomer on the platinum surface electrode. Then the monomer is oxidized with the loss of an electron and the formation of a cation radical. This step corresponds to the oxidation peaks observed in Figure 5. This step is followed by a deprotonation with formation of a radical, which dimerizes to the disulfide. Then, other sequences of oxidation, deprotonation, oligomerization take place yielding a polymer film. Therefore, a polyethylenedisulfide $(CH_2\text{-}CH_2\text{-}S\text{-}S)_n$ grows progressively on the electrode surface.
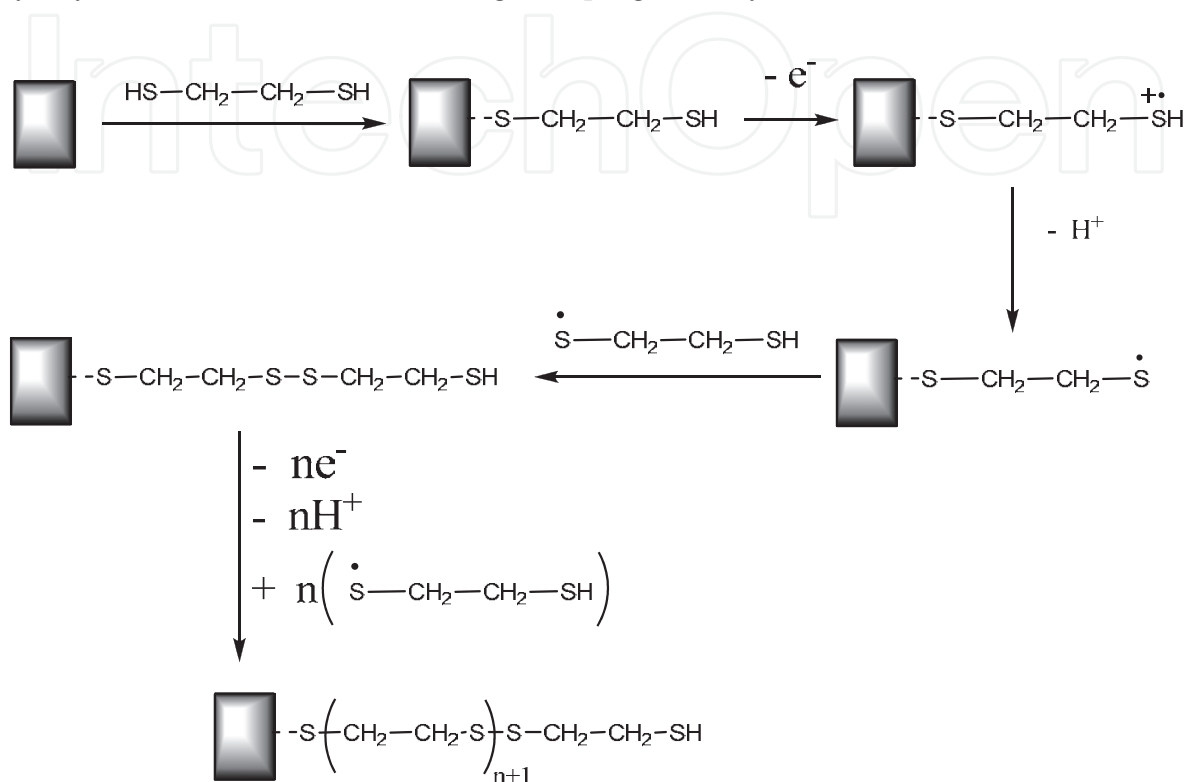

Fig. 11. Proposed mechanism of the anodic oxidation of EDT.

2.3 Anodic oxidation of glycine

The first electrochemical studies of amino acids date back to the 60 s and focused on their behavior in strong acid solutions where amino acids leads to carboxylic acids, aldehydes, ammonia and carbon dioxide (Lund et al., 1991). Electrochemistry of amino acids spread out until a renewal of interest at the end of the 90 s for studying the adsorption, reactivity and protein-surface interactions. From the literature, glycine has attracted extensive attention in recent years with investigations on single crystal electrodes (Huerta et al., 1997; Zhen et al., 2004) as well as on polycrystalline electrodes (MacDonald et al., 1997) due to its small size and chemical and biological importance. Many voltammetry studies on single crystal electrode coupled to several in situ techniques such as infrared (FTIRS) or Raman (Xiao et al., 2002) SERS spectroscopy and quartz crystal microbalance were performed. Different electrode materials were used. For instance, on monocrystalline electrode such as Pt(111) electrode, strongly bonded cyanide is formed above 0.5 V/RHE with CO_2 generation from the carboxyl group oxidation (Kolbe reaction). In addition, reversible adsorption of glycinate anions has been detected at potentials higher than 0.3 V. On Au(111) surface in alkaline solution, there is a dissociative adsorption of glycine leading to adsorbed cyanide from -0.6 to 0.0 V/SCE to give aurous cyanide at 0.3 V. Above 0.3 V several reactions may occur: (1)

direct oxidation of bulk glycine, (2) consumption of HO^- from H_2O hydrolysis for carbonate and bicarbonate formation and (3) gold atom dissolution from electrode surface.

For other electrode materials there are quite different results from some other works undertaken in the same period as those evocated previously. For instance, the anodic oxidation of glycine on glassy carbon electrodes (GCE) was carried out for elaborating amperometric sensors. The first application (Yu et al., 1997; Chen et al., 1997; Zhang et al., 2001) concerned the use of modified GCE from anodic oxidation of glycine $10^{-2}M$ dissolved in phosphate buffered solution of pH=7 for monitoring uric acid concentration. It was stated that the GCE was coated by polyglycine with no obvious proof, e. g. spectroscopic characterizations.

No data concerning the electrochemistry of highly concentrated glycine based electrolytes and their electrochemical behavior on smooth platinum electrode can be found. Indeed, the use of concentrated glycine solutions allow to enhance interaction between the electrode surface and their oxidation products.

Among usual solvents, only water dissolves glycine in great quantity. In our experiments the concentration was fixed to 0.5 M. Despite their electrochemical stability in a wide potential window, nonaqueous solvents such as propylene carbonate and N-methyl-pyrrolidinone were discarded because of the weak solubility reached in these solvents (less than 0.1 M). $NaBF_4$ 0.01 M was used as supporting electrolyte which is a salt with high solubility and high electrochemical stability. The different pH values of the electrolyte were adjusted either with H_2SO_4 or NaOH as needed.

EQCM experiments coupled to cyclic voltammetry technique were performed on smooth platinum electrode in aqueous solutions only. Due to the different forms that glycine can have (acidic, basic or zwitterion) as shown Figure 12, it was necessary to take into account the pH influence.

$$H_3\overset{+}{N}\text{-}CH_2\text{-}COOH \underset{H^+}{\overset{HO^-}{\rightleftharpoons}} H_2N\text{-}CH_2\text{-}COOH \overset{pH=6}{\longleftrightarrow} H_3\overset{+}{N}\text{-}CH_2\text{-}CO\overset{-}{O} \underset{H^+}{\overset{HO^-}{\rightleftharpoons}} H_2N\text{-}CH_2\text{-}CO\overset{-}{O}$$
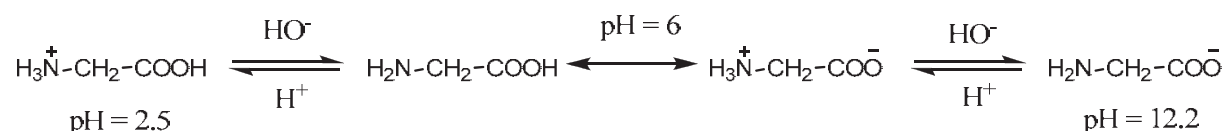
pH = 2.5   pH = 12.2

Fig. 12. The different glycine forms versus pH values

Different electrochemical studies were carried out at three different pH solutions which were 1, 6 and 13. Between 0 and 2.5 V vs. Ag^+/Ag as shown Figure 13, there is a faradaic peak corresponding to the glycine oxidation. Its potential position depends strongly on the pH value. The higher the pH, the higher the anodic oxidation potential E. The different peak potential values found are E=0.88 V at pH=1, E=0.95 V at pH=6 and E=1.70 V at pH=13.

The gravimetric curves obtained simultaneously allow correlating the mass variation at the electrode surface to the pH and the potential values (Figure 14). It can be seen that only at pH above 13 there is a drastic mass increase beyond the anodic peak potential at 1.7 V vs. Ag^+/Ag during the forward scan and the mass deposition goes on during the reverse scan. At pH=1, the slight mass increase that occurred beyond 0.55 V during the forward scan is totally cancelled during the reverse scan.

At pH=13 (above pKa=12.2) and between 1.4 and 1.9 V (Figure 15), there is a current drop with decreasing peak intensity as the scans proceed. No reverse peak is observed suggesting an irreversible reaction at the platinum surface that yields an insulating coating.
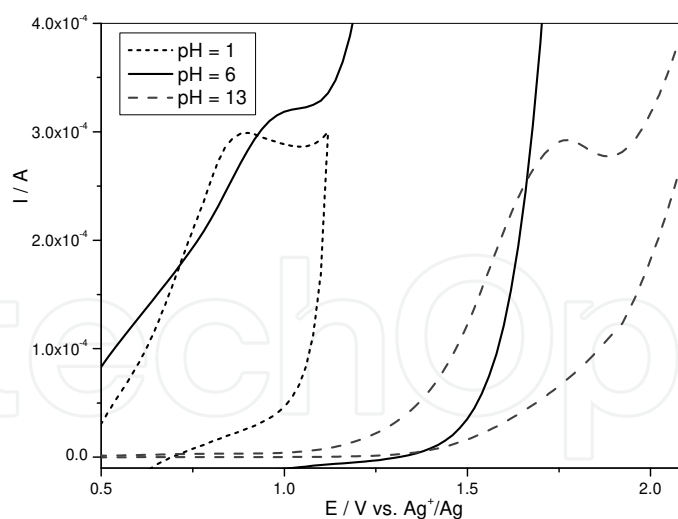
Fig. 13. Cyclic voltammogram of glycine 0.5 M in water at three different pH values. Scan rate: 20 mV/s.
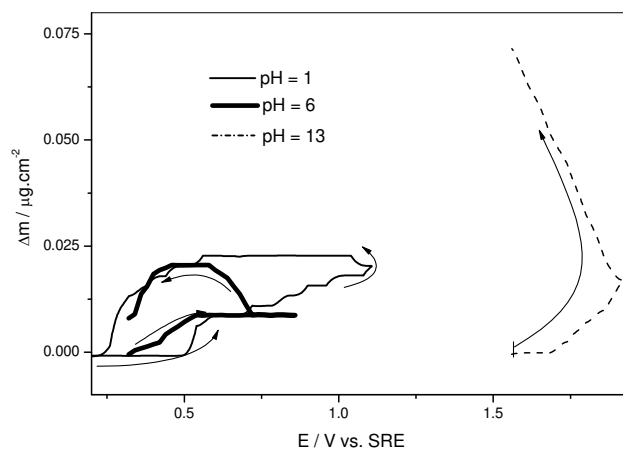

Fig. 14. Gravimetric curves coupled to cyclic voltammetry of glycine 0.5 M in water at three different pH values. Scan rate: 20 mV/s.
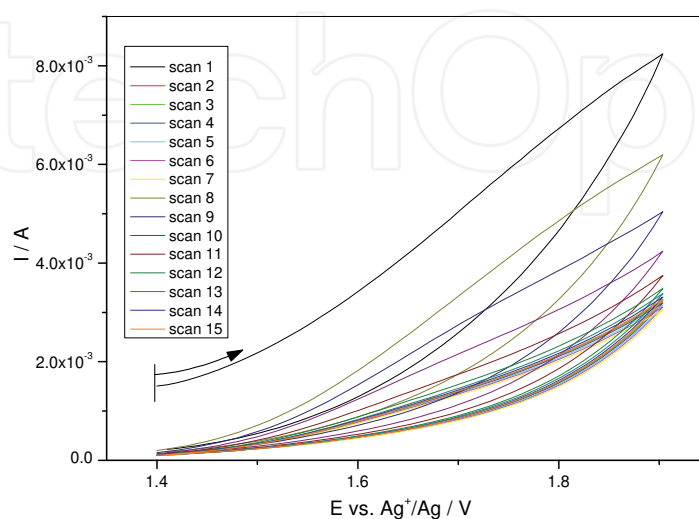

Fig. 15. Ten cyclic voltammograms of glycine 0.5 M in water at pH 13.
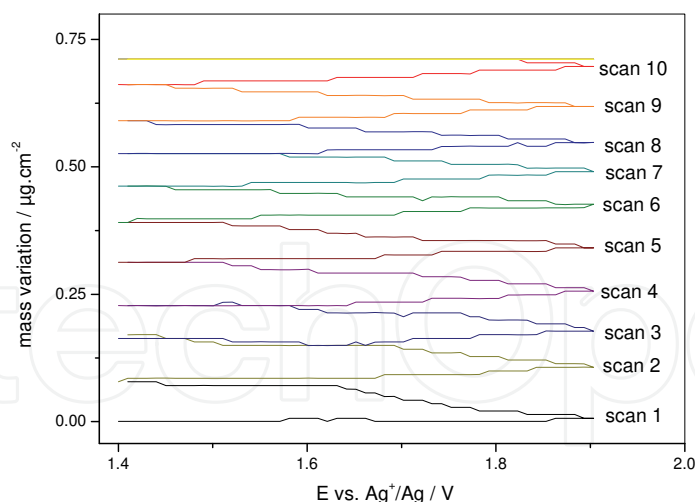
Fig. 16. The simultaneous gravimetric curves obtained with the EQCM.

Simultaneous EQCM measurements (Figure 16) show the constant mass increase at the platinum surface between 1.4 and 1.9 V vs. Ag^+/Ag as the scans proceed. It can be also noticed that the mass deposition is more important for the first scan than for the others.

The influence of glycine concentration on the mass electrodeposited at the electrode surface at pH = 13 shows that the mass increases with increasing concentration of glycine in a quite linear way up to 1 M. Before and after the electrochemical experiments, no pH change in the electrolyte solution is detected.

After ten scans, the electrode surface, rinsed with water, sonicated during 30 s and dried at 300 K, it is possible to distinguish with naked eye, a slight milky-white complexion.

Topographic AFM image Figure 17 shows a complete change compared to Figure 18 depicting the bare platinum surface. The typical platinum nodules (about 50 nm diameter) have disappeared suggesting an important thickness of the coating. We are not in presence of a monolayer of adsorbed species. In addition, the scare lines observed are characteristic of stick – slipping interactions between the tip and the coating denoting its polymeric structure.

ATR-FTIR spectra at air after electrochemical experiments at pH =1, 6 and 13 are very similar. Thus, only the spectrum of the coating performed at pH=13, which corresponds to the most abundant electrodeposited mass among the three pH values, is shown Figure 19. The anodic oxidation of concentrated glycine based electrolyte leads to a passivated electrode surface with a polypeptide coating. These peptide bond formations are probably electrocalysed during the anodic oxidation of primary amine in water. Effectively, the anodic oxidation of $R-CH_2-NH2$ in water yields aldehyde R-CHO. And the reaction between aldehyde and primary amine leads to amide. In addition, the ATR-FTIR spectra from our coatings are different from the glycine (or glycine salt) one (Rosado et al., 1998).

The spectral features of our coating displayed Figure 4 are almost identical to those of polyglycine II (PGII) oligomers (Taga et al., 1997). Due to the tight binding of our coating with the platinum surface, some vibration modes can disappear and some others can be enhanced, e.g. the amide III mode in the region 1290 - 1240 cm^{-1} and the primary amine at 1100 cm^{-1}, respectively. The presence of $-CH_2$ bending vibrations at 1450 – 1400 cm^{-1} is in favor of oligomers. But the characteristic skeletal stretching band for PGII (bulk) at 1027 cm^{-1} is not visible in our case since $-NH_2$ band is broad in this region.
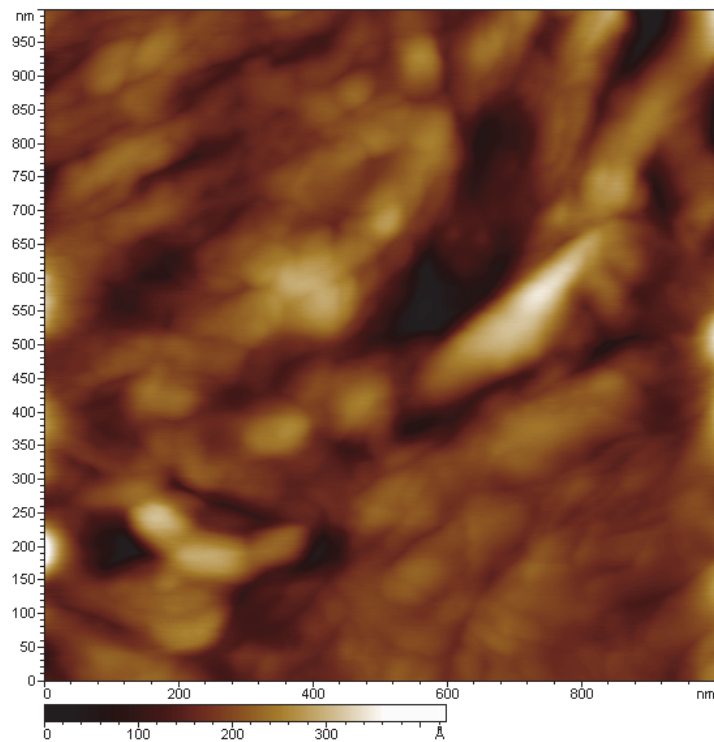
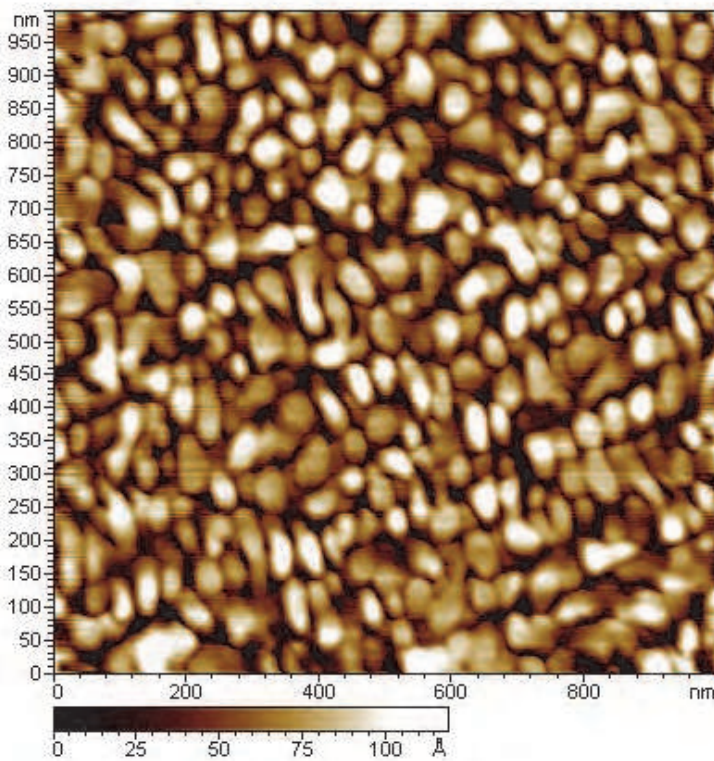Fig. 17. AFM topography in contact mode of the platinum coated quartz after 20 voltammetric sweeps.

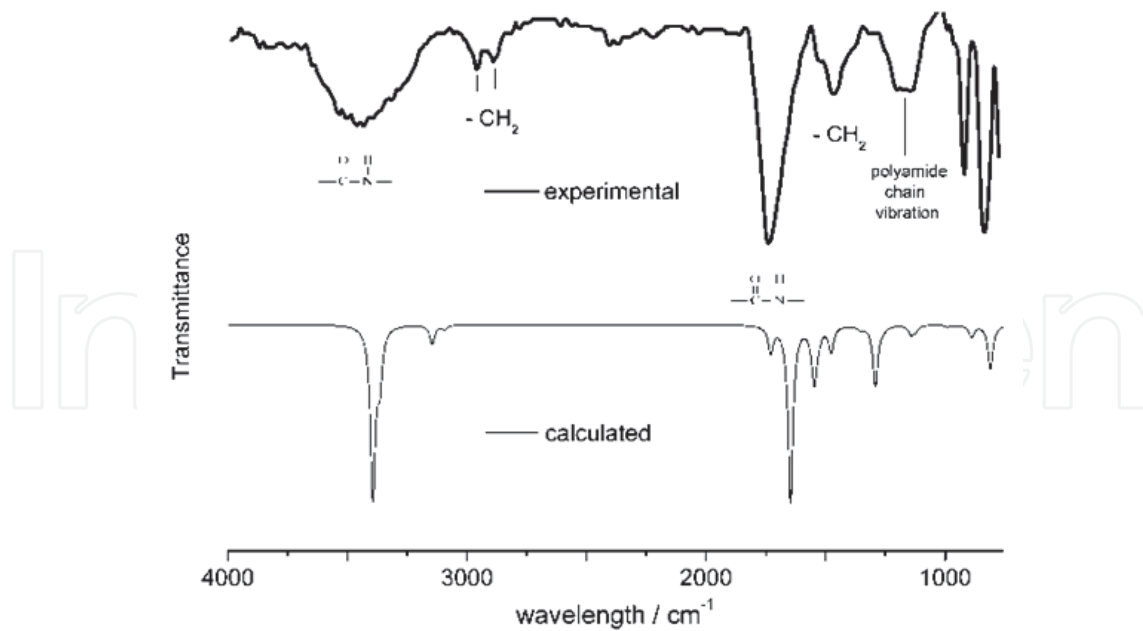Fig. 18. The bare platinum surface.

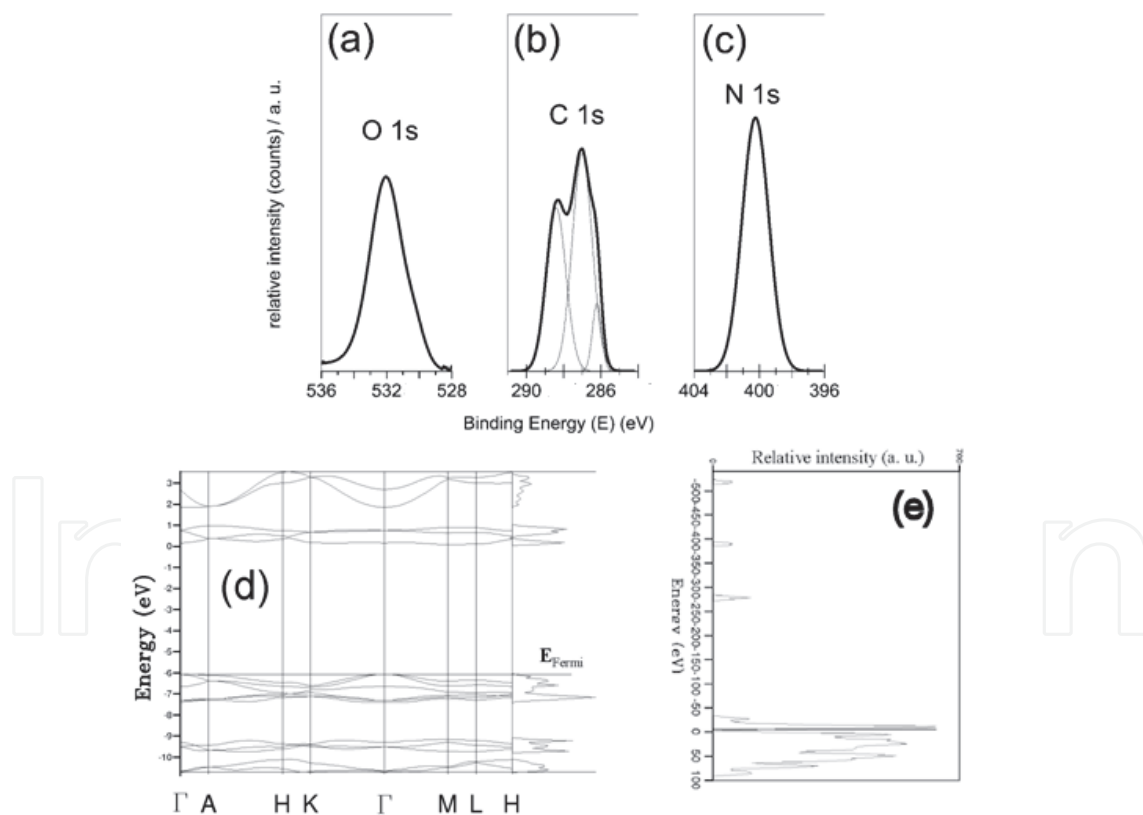Fig. 19. IR-ATR spectroscopy of anodic oxidation of glycine and theoretical spectrum

Fig. 20. xps spectroscopy of the anodic oxidation of glycine on Pt and calculated band structure and density of states.

The changes in the chemical environment of platinum surface were analyzed by XPS. If ATR-FTIR can detect chemical groups within few micrometers, XPS can probe only depth of ten nanometers. Figure 20 shows the XPS survey spectrum (a) and the C 1s (b), N 1s (c) and

(d) O 1s regions. The pre-peak at 5 eV in the onset in figure 5a is characteristic of a polymeric structure. Two C 1s peaks are clearly resolved Figure 20b. The peak at 285.5 eV can be attributed to -CH$_2$, while the other at 288.8 can be assigned to –C=O. The peak areas give a ratio of 1 –C=O for 2 –CH$_2$. The peak at 287.3 eV seems to be intrinsic to glycine system and remains unclear (Löfgren et al., 1997). As shown Figure 20c there is one asymmetric peak in the N 1s region. Peak deconvolution gave two different environments at 400.4 eV and 399.2 eV. The lowest energy binding corresponds to amide bond whereas the other at 400.4 eV is related to -(C=O)-NH-(CO)-. The IR band absorption of C=O in -(C=O)-NH-(CH$_2$)- is strong between 1670 and 1790 cm-1. There is effectively strong but large band absorption on the spectra in this wave number window. In these conditions, XPS is best suitable to analyze this coating. The Figure 20d in the O 1s region reveals two peaks at 531.8 eV and 536 eV. The asymmetric peak at 531.8 eV is attributed to –C=O in polyamide bond and the deconvoluted peak at 532.7 eV agrees well carboxylate energy binding. The peak at 536 eV remains unresolved.

The XPS data shown in Figure 20 are very different from those concerning glycine adsorbed on Pt(111) (18). Cyanide group is not present.

A possible mechanism can be proposed in the Figure 21 taking into account the chemisorption via the carboxylate group at pH=13, the anodic oxidation of primary amine that yields aldehyde and its reaction with amine from glycine leading to amide bond. This later step was deduced from XPS results and specifically that at 400.4 eV in the N 1s region. Further reactions with peptide formation lead to a product which looks like polyglycine composition.
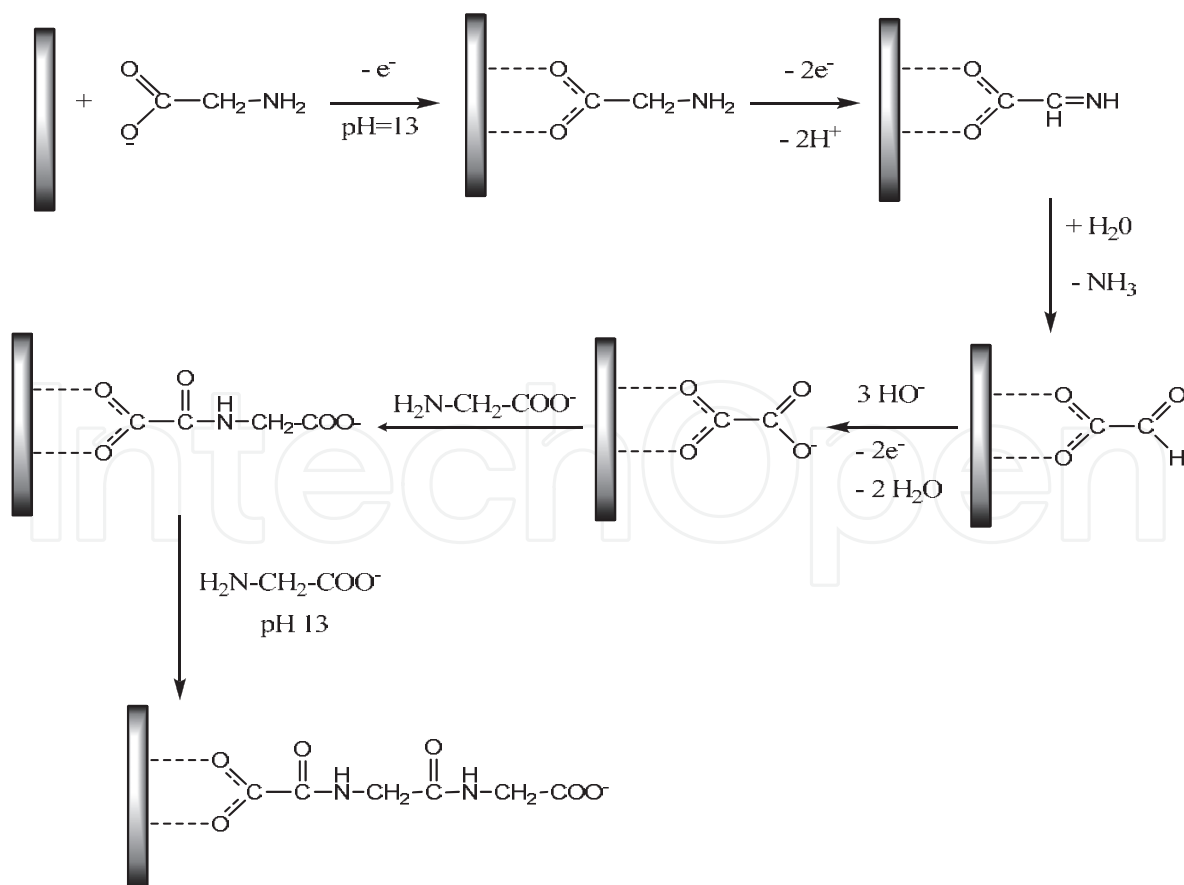

Fig. 21. Possible mechanism of the anodic oxidation of glycine leading to PG II.

2.4 Cathodic reduction of 3-aminopropyltriethoxy silane

The sol-gel process has been extensively investigated over the last twenty years especially to develop organically modified silicate (ormosils) films yielding the first industrial applications (Schmidt et al., 1988). The interest in sol-gel chemistry stems from the easy way to produce advanced materials with desirable properties including optics, protective films, dielectric and electronic coatings, high temperature superconductors, reinforcement fibers, fillers, and catalysts (Keefer et al., 1990). The very mild reaction conditions (particularly the low reaction temperatures) plus the possibility to incorporate inorganic and organic materials to each other led to a conceptually novel class of precursor materials.

Two years ago, the electrodeposition of trimethoxysilane (TMOS) on cathodically negatively biased conducting electrode surfaces to form thin silane films was reported (Deepa et al., 2003). Compared to spin-casting or dip coating methods, electrochemistry offers several advantages such as film thickness and porosity controls.

3-APTES which is among the most widely used chemicals in direct surface modification (Diao et al., 2005) based on silanization for biomolecule immobilization (Blasi et al., 2005), was rarely used until now for biosensor applications as chemically modified electrodes (Pauliukaite et al., 2005; Kandimalla et al., 2005). The present research seeks to explore on the basis of the Figure 1, the electrochemical behavior of pure or diluted nonaqueous 3-APTES based electrolytes for the preparation of ultra thin 3-APTES films on gold surfaces.

Many pure liquid state trialkoxyalkylsilanes exist as well as some organofunctional silanes such as 3-APTES. But due to their low dielectric constant (between 0.7 and 3) (Carré et al., 2003; Weast et al., 1968), they have never been regarded as solvents of interest in electrochemistry. $N(C_4H_9)_4PF_6$ dissolved in 3-APTES yields a conductivity of about 1 µS/cm at room temperature. The amino group presence in 3-APTES molecule does not enhance the salt solubility considerably as it is observed in pure 1,3-DAP where highly concentrated electrolytes can be reached up to 4M for instance.

Cyclic voltammetry (Figure 22) performed in 3-APTES charged with $N(C_4H_9)_4PF_6$ (10^{-3} M) plus freshly added water (10^{-3} M), between -4 V and 4 V versus Ag^+/Ag and shows neither net faradic peak nor gas evolving on the electrode surfaces (both working and counter electrodes). It can be observed thanks to EQCM experiment (Figure 23) coupled to cyclic
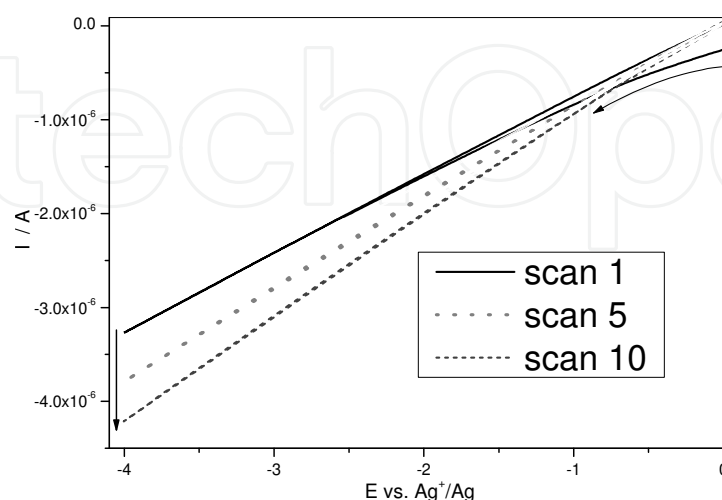

Fig. 22. Cyclic voltammogram in cathodic reduction of 3-APTES containing 1 mM of N(C4H9)4PF6 plus 1 mM of water.
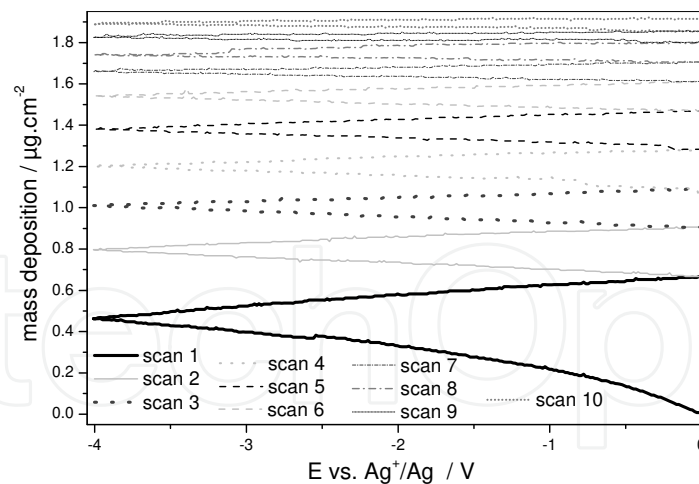
Fig. 23. Corresponding mass deposition as a function of the potential applied to a 5 MHz gold coated AT cut quartz crystal.

voltammetry that there is a mass deposition on gold electrode surface up to 2 μg.cm^{-2} at the end of the 10th scan according to the Lewis and Lu relationship (Lewis et al., 1972). This corresponds to a frequency change of 115 Hz which is in excellent agreement with the 5 MHz quartz crystal AT cut sensitivity of 56.6 Hz.cm^2.μg^{-1}. From the anhydrous 3-APTES based electrolyte (charged only with $N(C_4H_9)_4PF_6$) synthesized in a glove box under argon stream, no net mass deposition was observed on gold surface when biased cathodically but strong adsorption/desorption phenomena as a function of time occurs at zero current.

The electrochemical behavior of 3-APTES was also investigated in tetrahydrofurane (THF) because of the very negative cathodic wall reched in this solvent, and good solubilities of siloxane and ammonium salt (Lund et al., 1991). The electrogenerated hydroxide ions during the cathodic reduction process due to the water decomposition, acts as the catalyst for the hydrolysis and condensation of 3-APTES. Actually, amino groups are not reduced during this process. Figure 24 shows a cathodic voltammogram quite similar to that obtained Figure 22 without any reduction wave but showing a curve inflexion around -1.2 V
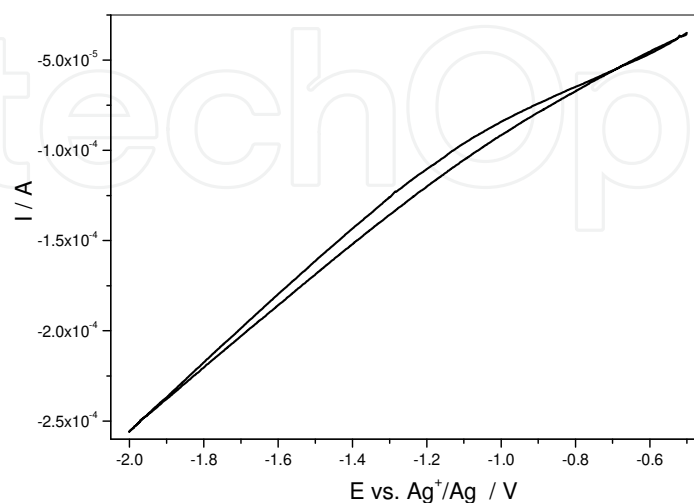

Fig. 24. Cyclic voltammogram of THF based electrolyte containing 1 mM of N(C4H9)4PF6 plus 1 mM of water.
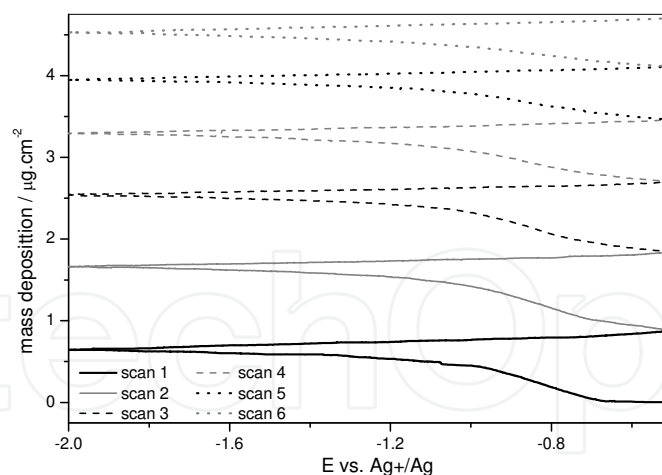
Fig. 25. Corresponding mass deposition as a function of the potential applied to a 5 MHz gold coated AT cut quartz crystal.

corresponding to the beginning of the cathodic limit of THF. Considering the mass variation curve recorded simultaneously (Figure 25) during cyclic voltammetry experiment, there was no need to go down to -4V and potential scans were limited in the potential range -0.5 to -2 V. Effectively, the mass deposition rate is optimum between -0.7 V and -1 V, evolving in an asymptotic manner beyond -1V as illustrated Figure 2b. At the end of the 10th scan, the mass deposition is more important than in pure 3-APTES electrolyte, reaching 4.7 $\mu g.cm^{-2}$. Clearly, 3-APTES has not to be concentrated in THF because the mass deposition is twice in THF based electrolyte than that in pure 3-APTES one and water concentration has to be in the same range.

The film thicknesses versus the biased electrode durations determined ex situ by ellipsometry measurements in air are reported Figure 26, as a function of cycles. There is a
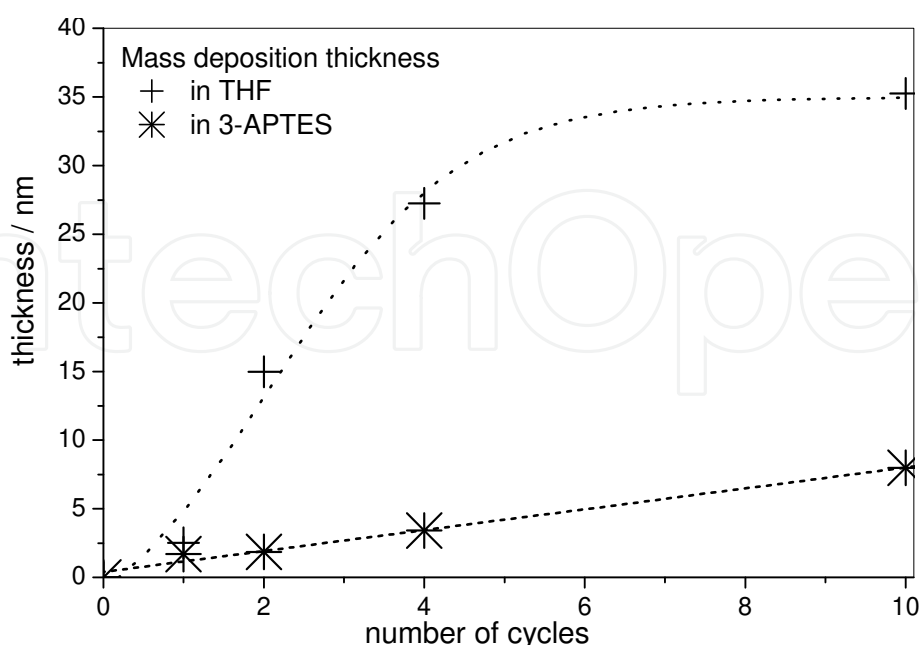

Fig. 26. 3-APTES layer thickness as a function of the number of cyclic voltammetry cycles in either 3-APTES based or THF based electrolytes.

noticeable difference, for the same potential range cycling [-0.5 to -2V], between the mass deposition in THF and in pure 3-APTES. The thickness versus the cycle numbers in THF based electrolyte is best fitted with a sigmoid curve, whereas in pure 3-APTES a linear regression matches very well the experimental data. Moreover, at the end of ten cycles the coating thickness is still growing up either in THF or in pure 3-APTES but of lesser importance than for the first cycles.

The IR-ATR characterization performed on the electrochemically modified gold coated quartz crystal in THF based electrolyte is given Figure 27 (raw spectra without any correction). The recorded spectrum of the pure 3-APTES shows typical absorption bands at 3374 cm^{-1} and 3282 cm^{-1} (νN-H for -NH$_2$), noteworthy is a considerable decrease in signal on gold surface. But IR-ATR enables us to detect -NH$_2$ groups despite the noisy band at about 1600 cm^{-1}. This noise is often observed at this frequency for IR-ATR spectra of electrodeposited linear polyethylenimine thin films from the anodic oxidation of ethylenediamine based electrolytes. The strong doublet at 1104 and 1084 cm^{-1} as well as the stronger band at 1022 cm^{-1} give evidence of the Si-OCH$_2$CH$_3$ presence. Between 1000 and 900 cm^{-1}, shoulders at 972 and 933 cm^{-1} are in favor of Si-O-metal formation.
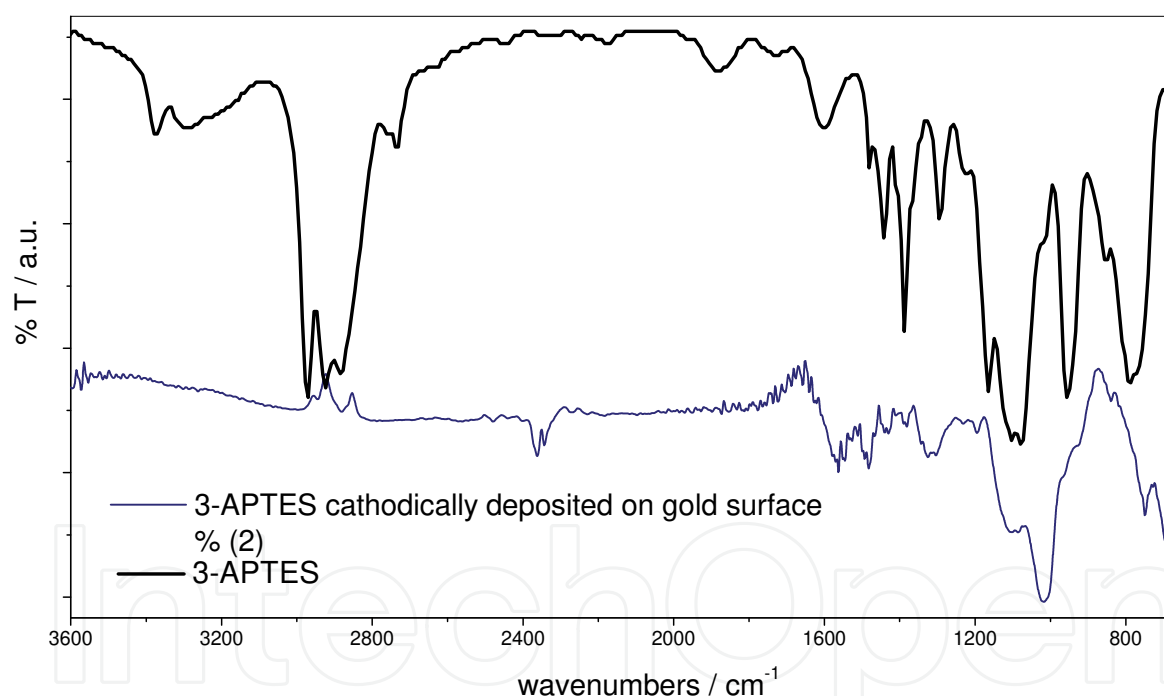

Fig. 27. FT-IR-ATR spectra of pure liquid 3-APTES and cathodic reduction of 3-APTES in THF on gold surface.

The topography and electrical properties of the 3-APTES thin film were examined with scanning tunneling microscopy. Figure 28a shows a typical STM image of freshly annealed Au(111) substrate; the presence of atomically flat Au(111) terraces over hundreds of nanometers. Figure 28b shows an image in water of the former gold substrate, biased between -0.5 and -2 V during one cycle in THF based electrolyte, where dot coverage takes place with a high density. When biased between -0.5 and -2 V during three cycles in THF based electrolyte, Figure 28c, the gold substrate is uniformly passivated. In fact, it was

impossible to image the 3-APTES coating at this stage in water but only in air (with difficulty). For this reason and as many insulating thin film coatings, 3-APTES ensure uniform thickness coatings without pinhole.
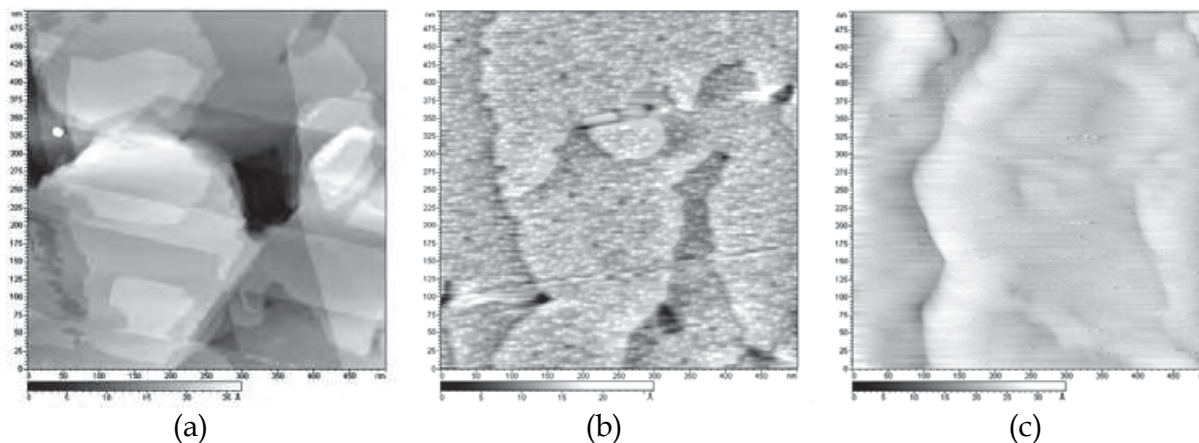

(a)   (b)   (c)
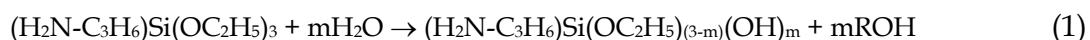
Fig. 28. STM picture recorded in (a) air of freshly annealed Au(111) on mica; (b) water of cathodically electrodeposited 3-APTES between -0.5 and -2V during one cycle at 20 mV/s in THF based electrolyte and (c) in air of cathodically electrodeposited 3-APTES during three cycles at 20 mV/s between -0.5 and -2V in THF based electrolyte.

The possible reactions of the cathodic reduction of water are

$$2\,H_2O + 2e_- \rightarrow 2\,HO^- + H_2$$

$$O2 + 2\,H_2O + 4e^- \rightarrow 4\,HO^-$$

$$O2 + 2\,H_2O + 2e^- \rightarrow H_2O_2 + 2\,HO^-$$
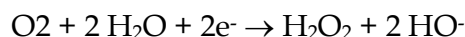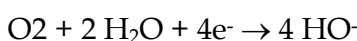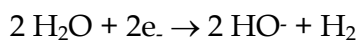
The hydrolysis of 3-APTES (1) and its condensation (2) on the hydroxyl covered surface HO-| lead to the following mechanisms :

$$(H_2N\text{-}C_3H_6)Si(OC_2H_5)_3 + mH_2O \rightarrow (H_2N\text{-}C_3H_6)Si(OC_2H_5)_{(3\text{-}m)}(OH)_m + mROH \quad (1)$$

$$(H_2N\text{-}C_3H_6)Si(OC_2H_5)_{(3\text{-}m)}(OH)_m + HO\text{-}| \rightarrow (H_2N\text{-}C_3H_6)Si(OC_2H_5R)_{(3\text{-}m)}(OH)_{(m\text{-}1)}\text{-}O\text{-}| + H_2O \quad (2)$$

In summary, gold surfaces can be modified electrochemically from the cathodic reduction of 3-APTES. This siloxane is not only grafted covalently to gold metal via oxo bond but is also electrodeposited over several nanometer thicknesses on gold surface suggesting a multilayer coating. Electrochemical studies of 3-APTES based electrolytes showed that gold surface modification is irreversible and mass deposition is larger in THF than in 3-APTES based electrolyte. In addition, the deposition catalyzed electrochemically in presence of water occurs on different electrode material such as Pt, Ti, glassy carbon, etc.

3. Insulating polymer thin film based biosensors

Immobilized enzyme on electrode surface is of prime importance when used as biosensors since their selectivity and selectivity for analyte detection. Molecule recognition requires also a good accessibility of the enzyme catalytic site. Consequently the simpler the enzyme attachment is, the more efficient the biosensor is. Until now, several solutions were

developed for immobilizing enzyme onto a surface using rather chemical protocols in water (Cosnier et al., 1999) than possibilities supplied by nonaqueous chemistry and/or electrochemistry which remain in great part unexplored (Kröger et al., 1998; Dumont et al., 1996).

The electrochemical deposition of thin film polymers presented previously allows directly and in one step the covalently grafting of films belonging functional groups of interest on metallic (Au, Pt, Fe, Ti, glassy carbon) or semiconducting surfaces (Si-p type, fluorine doped tin oxide). This part illustrates how to take advantage of the functional group presence in the thin film coatings presented previously for sensor and biosensor applications following the scheme displayed in Figure 29.
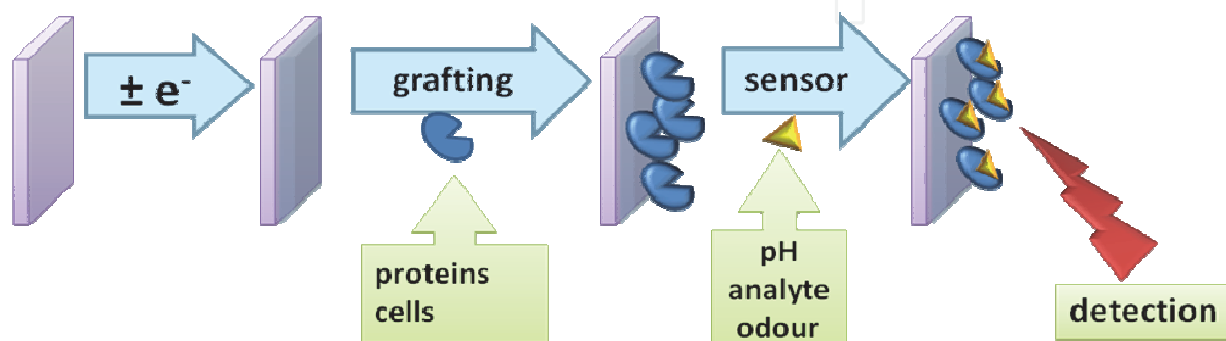
Fig. 29. general scheme of a thin film coating based (bio)sensor.

3.1 pH and ion sensors

The covalent grafting of amine based thin films on the electrode surface and their affinity towards protons makes them good candidates for pH receptor. PG behavior as pH sensor is compared to L-PEI and polyaniline (PANI).

In this purpose, the realization of a micro-sensor composed of two microelectrodes (Pt: working electrode; Ag^+/Ag: reference electrode) deposited on a glass substrate (Figure 30) was achieved via a conventional photolithography process (Figure 31).
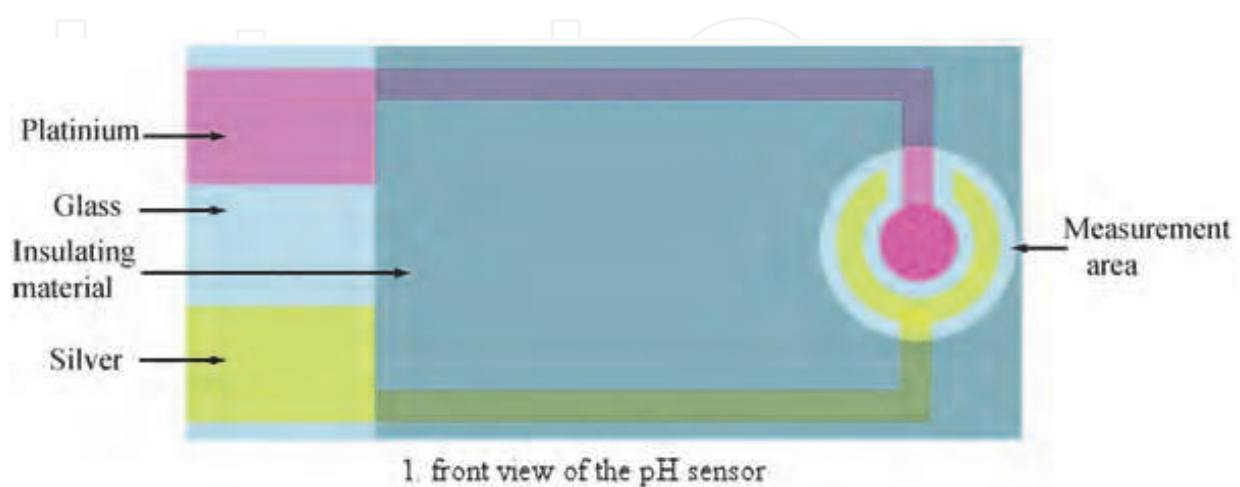
1. front view of the pH sensor

Fig. 30. pH sensor with two electrodes: a thin film based Pt electrode and a reference electrode (silver).

Photoresist

Glass

1 . Spin coating of the photoresist.

2 . Developpement of the photoresist.

UV

Mask

3 . Exposure to UV light through the mask.

Ti/Pt or Ti/Ag

4 . E-beam evaporation of the metals.

UV

5 . Second exposure to UV light without
mask after baking.
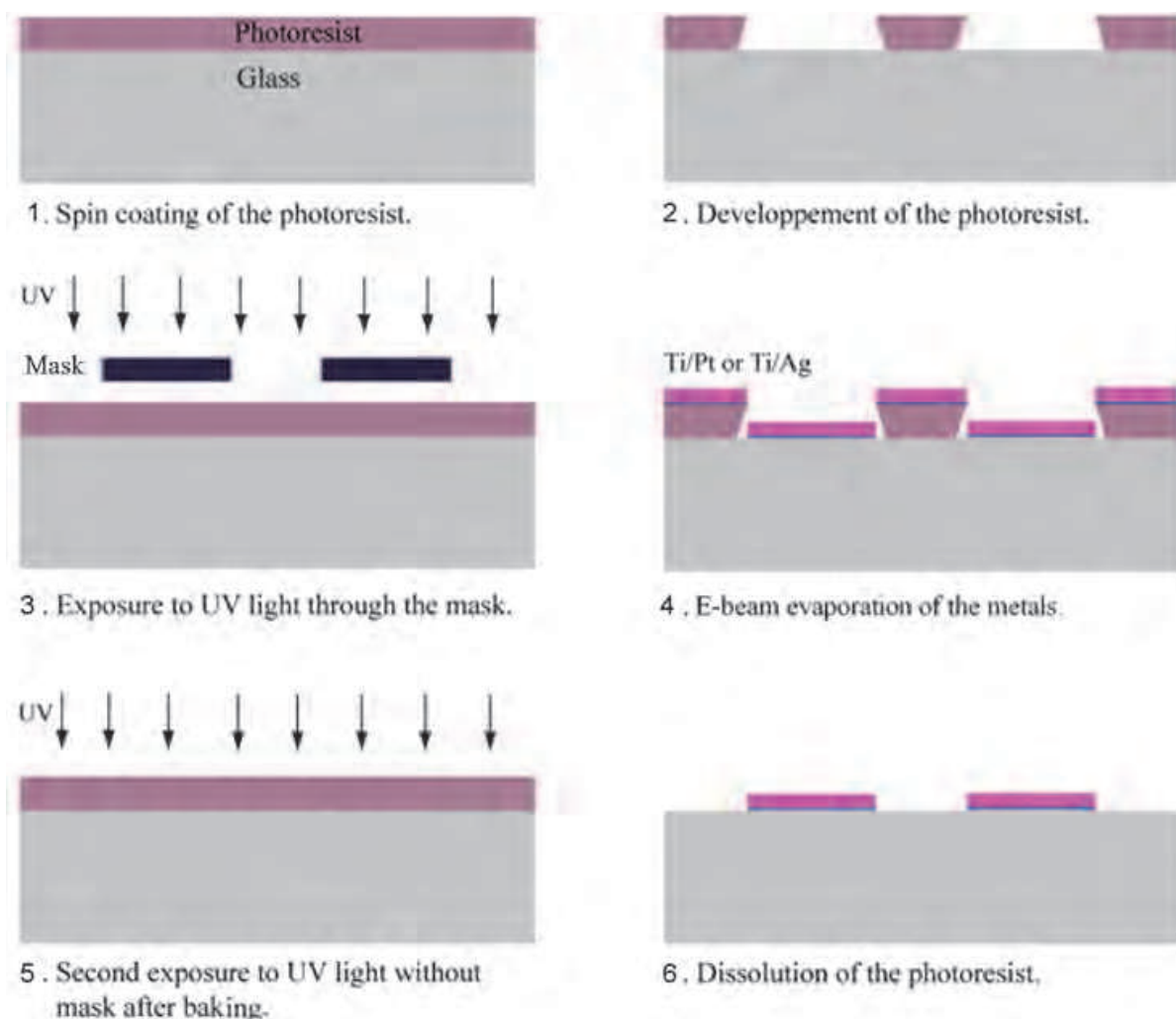
6 . Dissolution of the photoresist.

Fig. 31. Photolithography process of the pH sensor

The microelectrode connexions have rectangular ends which can be plugged to the digital voltmeter. The pH sensor architecture has been chosen for studying the effect of the geometry (diameters of the working electrode: 1000, 500, 125 and 10 μm) and to optimize the interaction between the two electrodes. A silica layer is deposited at the final step on the substrate excepted on the measuring area and the two ends allowing an effective electrical insulation. Thus, only the measure areas (Pt and AgCl) are in contact with the solution.

According to the works described previously, different thin polymer films (PGII, L-PEI and PANI) on smooth Pt were electrodeposited by cyclic voltammetry: ten scans are sufficient to coat irreversibly the platinum surface for PG and L-PEI modified electrodes whereas two scans are carried out for PANI. The resulting coatings, due to the amino group presence, act as proton receptors where the variation of the charge density occurs depending on the proton concentration.

The Pt/PG modified electrodes were tested in potentiometric mode as pH receptor when dipped in different buffered solutions at 293 K. In all the cases, there are large potential variations in the considered pH range. For PGII coating (Figure 32a), at the millimeter scale the potentiometric response is quasi Nernstian (52.4 mV/pH) but decreases down to 41.1 mV/pH for 10 μm electrode size which is a loss of sensitivity of about 20%. Despite this smaller sensitivity, pH measurements are still possible and reliable with a 10 μm electrode size.
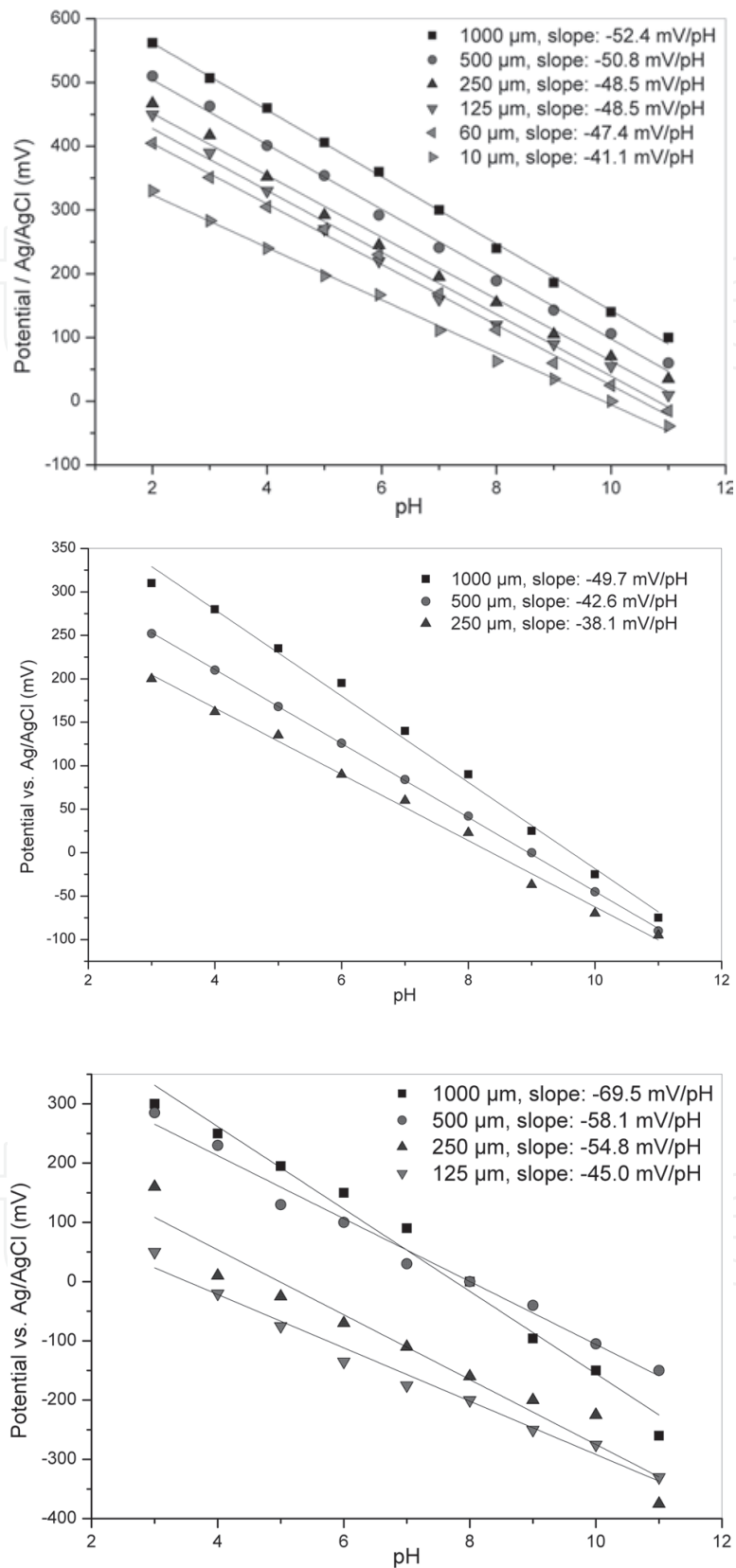
Fig. 32. pH measurements on Pt electrode of different sizes in the pH range: (a) for Pt/PG, (b) for Pt/PEI-L and (c) for Pt/PANI.

Concerning Pt/L-PEI electrodes, the same trends can be observed as for Pt/PG ones since L-PEI but is stable in a narrower pH range [3- 11] than that of PG (Figure 32b). Compared to Pt/PG and Pt/PEI-L, Pt/PANI (Figure 32c) modified electrodes have quasi to sub Nernstian (69.5 mV/pH) behaviors, depending on the electrode size. In fact, the potential response characterizes not only the transduction of proton concentration vs. pH but also the redox sensitivity of PANI to ionic species in the buffered solutions. This chemical environment can lead to doped PANI that switches to conducting state, yielding in return side electrochemical reactions responsible for over voltage and then sub Nernstian response. Another drawback in using this redox polymer is its tendency to peel off in acidic medium.

Response time of the pH measurements, linear relationship between pH and electrode potential, and the reproducibility are also important factors to take into account. Concerning the reversibility of the potentiometric measurements versus pH, the equilibrium potential response time decreases with the decreasing electrode size. In fact, at least two parameters are essential at this stage: the thickness of the polymer coating and the electrode area. Ellipsometric measurements have shown that after the electrodeposition process described previously, the PG coating thickness is around 15 nm (Table 2). Beyond this thickness value, the response time is increased and below, the pH sensitivity is decreased. The smaller the electrode size, the smaller the sensitivity (slope). For instance, at the millimeter size, the response time is about 30 s and less than 10 s for 10 μm electrode size. The response time which is comparable to that of a glass pH electrode with millimeter size electrode (30 s), is shorten drastically at the micrometer scale. We adjusted the parameters for the other electropolymerization process in order to have polymer thickness for PEI-L and PANI in the same range than that of PG.

The reversibility of the pH measurement is directly related to the response time. Reversible tests on Pt/PG with 10 μm diameter electrode were made by comparing the potential responses after a pH scan from 2 to 11 and return to 2. No noticeable difference was detected. For Pt/PEI-L and Pt/PANI, the difference is barely noticeable with 10 μm electrode size too. Globally, the potential variations vs. pH of all the modified electrodes present a linear response. The linear correlation coefficients are near 1 for Pt/PG and Pt/PEI-L modified electrodes and between 0.93 and 0.98 for Pt/PANI.

The ageing of the Pt/PG electrode was examined by testing the responses of a newly prepared Pt/PG 60 μm size over a period of thirty days. The sensitivity of this system is slightly decreased to 42 mV/pH unit with a potential shift of +120 mV, which is suitable for monitoring the pH in the range [2 – 12]. Notice that the ageing of PANI [13] has a large impact on its electronic properties which is not in favor of its use as pH transducer for a long period of time.

Electrodeposited polymer	Number of cycles (cyclic voltammetry)	Thickness (nm)
PG II	10	15 ± 0.4
L-PEI	10	18 ± 0.4
PANI	2	50 ± 1

Table 2. Polymer thickness versus the number of cycles (cyclic voltammetry).

3.2 Biosensors

Bare gold surfaces from Biacore can be electrochemically modified with 3-APTES when biased negatively below –0.7V/SRE. The resulting polysiloxane film is coated covalently to gold metal via oxo bridges. The interest of such surface covered with amino groups is its grafting (cross-linking) thereafter biological molecules in mild conditions. As an example, α-lactalbumin was grafted on the 3-APTES based film electrodeposited on a bare gold chip (corresponding to 2 CV cycles deposition from the Figure 25). This reaction was monitored by means of the SPR shift (Figure 33). After rinsing with distilled water (quoted 1 on the graph), 1% glutaraldehyde was injected on the surface (arrow A) during 1400 s (quoted 2). The sensor chip was rinsed three times with water (quoted 1) and α-lactalbumin (2mg/mL) was injected on the 3-APTES surface (arrow B) during 1700 s (quoted 3). The injection of - lactalbumin is then stopped (arrow C) and the difference in resonance units before and after α-lactalbumin injection corresponded to the amount of protein covalently attached to the 3-APTES surface (quoted 4). This result confirms that primary amino groups on the top of the 3-APTES thin film are available for covalent binding of proteins. Furthermore, the electrodeposited 3-APTES thin film on gold surface for SPR experiments allows graft and detection of macromolecules such as α-lactalbumin.
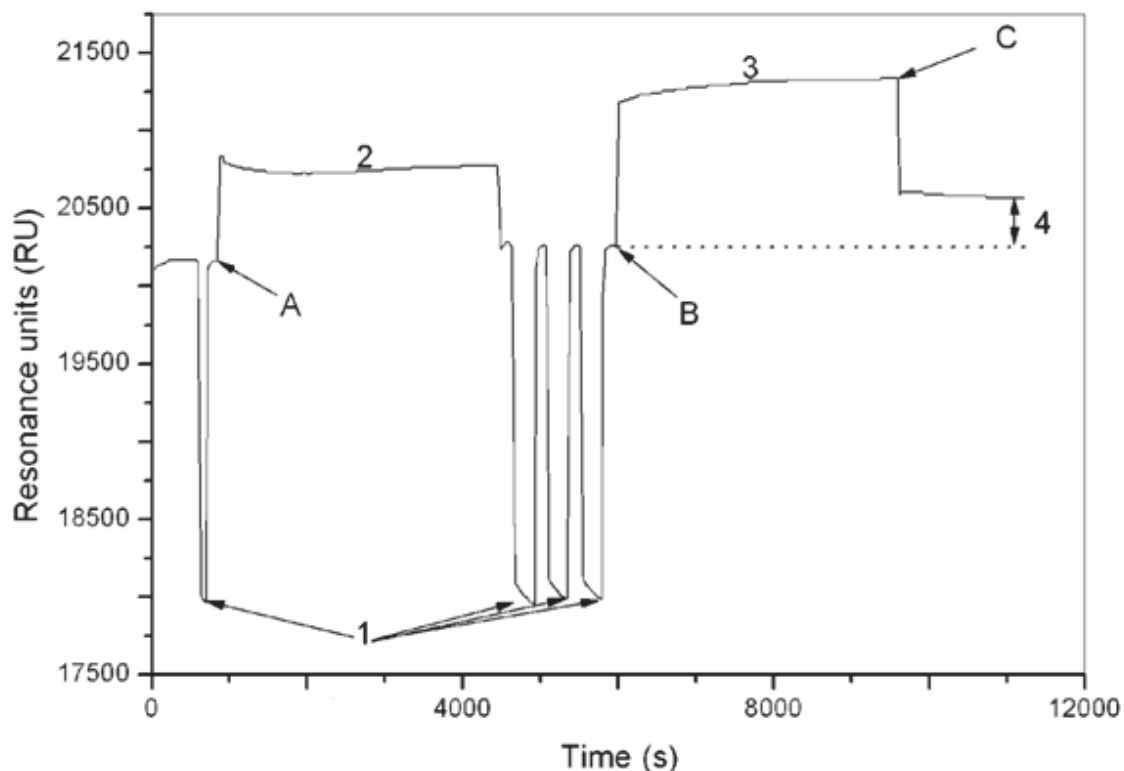

Fig. 33. SPR sensorgram from Biacore 3000 illustrating the binding of α-lactalbumin to electrodeposited 3-APTES on bare gold. The surface was first rinsed with water (1), then 1% glutaraldehyde (2) and α-lactalbumin at 2 mg/mL (3) were injected on the surface. Difference in resonance units before and after α-lactalbumin injection (4) corresponds to the amount of this protein covalently attached to the 3-APTES surface.

4. Outlook

The present review describes a new way for synthesizing thin film coatings from aliphatic bifunctional monomer, their characterization and their use as tranducers for sensor and biosensor applications. These thin film coatings can be electrosynthsized during anodic oxidation experiments (EDA, 1,3-DAP, DETA, 1,2-EDT, glycine) or during cathodic reduction (3-APTES).

The electrochemical synthesis of such polymers offers some advantages over chemical oxidation of aziridine or oxazoline for instance because on the electrode surface, the polymer is directly deposited and the adhesion creates tight binding allowing further grafting.

Although it has been shown the interest of such electropolymerization reactions, the combinations proposed Figure 1 can be continued with other functional groups such as alcohol, etc. It is possible by this way to explore deeply the scope of thin film coatings and use them in sensor and biosensor applications.

5. References

Adhikari, B.; Majumdar, S. (2004). Polymers in sensor applications. Progress in Polymer Science Vol.29, No.7, pp. 699-766.

Kalimuthu, P.; John, SA. (2009). Electropolymerized film of functionalized thiadiazole on glassy carbon electrode for the simultaneous determination of ascorbic acid, dopamine and uric acid. Bioelectrochemistry, Vol.77, No.1, pp. 13-18.

Granqvist, CG. (2007). Solar Energy Materials and Solar Cells, Vol.91, No.17, pp. 1529-1598.

Xiao, L.; Wildgoose, GG.; Compton, RG. (2009). Exploring the origins of the apparent "electrocatalysis" observed at C-60 film-modified electrodes. Sensors and Actuators B: Chemical, Vol.138, No.2, pp. 524-531.

Merkoci, A. (Ed) (2009). Biosensing using nanomaterials, ISBN: 978-0-470-18309-0, Wiley.

Medrano-Vaca, MG.; Gonzalez-Rodriguez, JG.; Nicho, ME.; Casales, M.; Salinas-Bravo, VM. (2008). Corrosion protection of carbon steel by thin films of poly (3-alkyl thiophenes) in 0.5 M H_2SO_4. Electrochimica Acta, Vol.53, No.9, pp. 3500-3507.

Liu, B.; Chen, X.; Fang, D.; Perrone, A.; Pispas, S.; Vainos, NA. (2010). Environmental monitoring by thin film nanocomposite sensors for cultural heritage preservation. J. Alloys and Compounds, Vol.504, No.1, pp. S405-S409.

Reiter, J; Krejza, O.; Sedlaříková, M (2009). Electrochromic devices employing methacrylate-based polymer electrolytes. Solar Energy Materials and Solar Cells, Vol.93, No.2, pp. 249-255.

Herlem, G.; Fahys, B.; Herlem, M.; Penneau, JF. (1999). A new relation between the maxima conductivities of nonaqueous concentrated electrolytes and chemical hardness of solvents and salts. J. Sol. Chem., Vol.28, No.3, pp. 223–235.

Herlem, G.; Reybier, K.; Trokourey, K; Fahys, B. (2000). Electrochemical oxidation of ethylenediamine: New way to make polyethyleneimine-like coatings on metallic or semiconducting materials. J. Electrochem. Soc., Vol.147, No.2, p. 597.

Saegusa, T., Ikeda, H., Fujii, H. (1972). Crystalline polyethylenimine. Macromol., Vol.5, pp. 108.

Biçak, N.; Senkal, BF. (1998). Removal of nitrite ions from aqueous solutions by cross-linked polymer of ethylenediamine with epichlorohydrin, Reactive & Functional Polymers Vol.36, No.1, pp. 71-77.

Aldrich FT-IR Handbook, Milwaukee, USA (1997).

Beamson, G.; Briggs, D. (1992). High Resolution XPS of Organic Compounds, The Scienta ESCA300 Database, pp. 182-183, Wiley Interscience.

Dick, CR.; Ham, GE. (1970). Characterization of polyethylenimine, J. Macromol. Sci. Chem., Vol.A4, p. 1301.

Gembitskii, PA.; Kleshcheva, NA. , Chhmarin, AI.; Zhuk, DS. (1978). Polymerization of ethylenimine to linear polyethylenimine. Polum. Sci. USSR (Engl. Trans.) Vol.A20, 2982 (1978).

Lakard, B.; Herlem, G.; Fahys, B. (2002). Ab initio study of the electrochemical polymerization mechanism leading from DETA to PEI, J. Mol. Struct. (Theochem), Vol.593, pp. 133–141.

Mann, CK.; Barnes, KK. (1970). Electrochemical Reactions in Non Aqueous Systems, Chapt. 8, p. 271, Dekker, NewYork, USA.

Lakard, B.; Herlem, G., Fahys, B. (2008). Electrochemical polymerization of 1,2-ethanedithiol as a new way to synthesize polyethylenedisulfide, Polymer, Vol.49, No.7, pp. 1743–1747.

Svensmark, BO; Hammerich, O (1991). Organic electrochemistry, 3rd edition. Lund, H; Baizer, MM (Eds), Dekker, New York, USA, ISBN 0-8247-8154-6; pp. 660-698.

Lund, H; Baizer MM. (1991). Organic Electrochemistry, 3rd edition, Lund, H; Baizer, MM (Eds), Dekker, New York, USA, ISBN 0-8247-8154-6, p. 601 and 3 references therein (1991).

Huerta, F., Morallón, E., Cases, F., Rodes, E; Vásquez, JL; Aldaz, A. (1997). Electrochemical behaviour of amino acids on Pt(h,k,l): A voltammetric and in situ FTIR study .1. Glycine on Pt(111). J. Electroanal. Chem., Vol.421, pp. 179-185.

Zhen, CH.; Sun, SG.; Fan, CJ.; Chen, SP.; Mao, BW.; Chen, YP. (2004). In situ FTIRS and EQCM studies of glycine adsorption and oxidation on Au(111) electrode in alkaline solutions, Electrochem. Acta, Vol.49, pp. 1249-1255.

MacDonald, SM.; Roscoe, SG. (1997). Electrochemical oxidation reactions of tyrosine, tryptophan and related dipeptides, Electrochem. Acta, Vol.42, No. 8, pp. 1189-1200.

Xiao, XY.; Sun, SG.; Yao, JL.; Wu, QH; Tian, ZQ. (2002). Surface-enhanced Raman spectroscopic studies of dissociative adsorption of amino acids on platinum and gold electrodes in alkaline solutions, Langmuir, Vol.18, 6274-6279.

Yu, AM.; Zhang, HL.; Chen, HY. (1997). Catalytic oxidation of uric acid at the polyglycine chemically modified electrode and its trace determination, Analyst, Vol.122, pp. 839-841.

Chen, HY.; Yu, AM.; Zhang, HL. (1997). Electrocatalytic oxidation of dopamine at the polyglycine chemically modified carbon fibre bundle electrode and its voltammetric resolution with uric acid, Fresenius J. Anal. Chem., Vol.358, pp. 863-864

Zhang, L.; Lin, X. (2001). Covalent Modification of Glassy Carbon Electrodes with Glycine for Voltammetric Separation of Dopamine and Ascorbic Acid, Fresenius J. Anal. Chem, Vol.370, pp. 956-962.

Rosado, M.; Duarte, MLTS; Fausto, R. (1998), Vibrational spectra of acid and alkaline glycine salts Vibrational Spectroscopy Vol.16, No.1, p.35-54.

Taga, K.; et al. (1997). Vibrational analysis of 3-chloropropylsilane, Vibrational Specroscopy Vol.14, No.2, pp. 143-146.

Löfgren, P. (1997), Glycine on Pt(111): A TDS and XPS study, Surface science Vol.370, 277.

Schmidt, H.; Seiferling, B.; Philipp,G.; Deichmann, K. (1988). Ultrastructure Processing of Advanced Ceramics, J. MacKenzie, D. & Ulrich, DR. (Eds), J. Wiley & Sons, Chichester, p. 651.

Keefer, KD (1990). Silicon Based Polymer Science: A Comprehensive Resource; Zeigler, JM. & Fearon, FWG., ACS Advances in Chemistry Ser. , American Chemical Society, Washington, DC, USA, No.224, p. 227.

Deepa, PN., Kanungo, M.; Claycomb, G.; Sherwood, PMA, Collinson, MM. (2003). Electrochemically deposited sol-gel-derived silicate films as a viable alternative in thin-film design, Anal. Chem., Vol.75, No.20, p. 5399-5405.

Diao, J.; Ren, D.; Engstrom, J. R.; Lee, K. H. (2005); A surface modification strategy on silicon nitride for developing biosensors, Anal. Biochem., Vol.343, No.2, pp. 322-328.

Blasi, L.; Longo, L.; Vasapollo, G.; Cingolani, R.; Rinaldi, R.; Rizzello, T.; Acierno, R.; Maffia, M. (2005). Characterization of glutamate dehydrogenase immobilization on silica surface by atomic force microscopy and kinetic analyses, Enzyme and Microbial Technology, Vol.36, No.5-6, pp. 818-823.

Pauliukaite, R.; Brett, CMA. (2005). Characterization of novel glucose oxysilane sol-gel electrochemical biosensors with copper hexacyanoferrate mediator, Electrochimica Acta, Vol.50, No.25-26, pp. 4973-4980.

Kandimalla, VB; Tripathi, VS.; Ju, H. (2006). A conductive ormosil encapsulated with ferrocene conjugate and multiwall carbon nanotubes for biosensing application, Biomaterials, Vol.27, No.7, pp. 1167-1174.

Carré, A.; Lacarrière, V; Birch, W (2003). Molecular interactions between DNA and an aminated glass substrate, J. Colloid and Interface Science, Vol.260, pp. 55.

Weast, RC. (Ed.) (1968). Handbook of chemistry and physics, E60, 49th edition, , the chemical rubber co.

Lewis, O.; Lu, C. (1972). Investigation of film-thickness determination by oscillating quartz resonators with large mass load, J. Appl. Phys., Vol.43, pp.4385.

Lund, H.; Baizer MM. (Eds) (1991). Organic Electrochemistry: an introduction and guide-3rd edition, ISBN 0-8247-8154-6, Marcel DEKKER Inc., p. 856.

Cosnier, S. (1999). Biomolecule immobilization on electrode surfaces by entrapment or attachment to electrochemically polymerized films. A review, Biosensors & Bioelectronics Vol.14, pp. 443-456.

Kröger, S.; Setford, SJ.; Turner, APF. (1998). Assessment of glucose oxidase behaviour in alcoholic solutions using disposable electrodes, Anal. Chim. Acta Vol.368, pp. 219-231.

Dumont, J.; Fortier, G. (1996). Behavior of glucose oxidase immobilized in various electropolymerized thin films, Biotechnology and Bioengineering Vol.49, pp. 544-552.
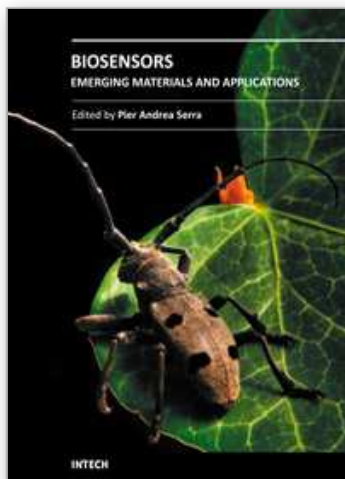
Biosensors - Emerging Materials and Applications

Edited by Prof. Pier Andrea Serra

ISBN 978-953-307-328-6

Hard cover, 630 pages

Publisher InTech

Published online 18, July, 2011

Published in print edition July, 2011

A biosensor is a detecting device that combines a transducer with a biologically sensitive and selective component. Biosensors can measure compounds present in the environment, chemical processes, food and human body at low cost if compared with traditional analytical techniques. This book covers a wide range of aspects and issues related to biosensor technology, bringing together researchers from 19 different countries. The book consists of 27 chapters written by 106 authors and divided in three sections: Biosensors Technology and Materials, Biosensors for Health and Biosensors for Environment and Biosecurity.

How to reference

In order to correctly reference this scholarly work, feel free to copy and paste the following:

Tijani Gharbi and Guillaume Herlem (2011). Electrodeposition of Insulating Thin Film Polymers from Aliphatic Monomers as Transducers for Biosensor Applications, Biosensors - Emerging Materials and Applications, Prof. Pier Andrea Serra (Ed.), ISBN: 978-953-307-328-6, InTech, Available from: http://www.intechopen.com/books/biosensors-emerging-materials-and-applications/electrodeposition-of-insulating-thin-film-polymers-from-aliphatic-monomers-as-transducers-for-biosen

INTECH
open science | open minds